Optimal Impedance Control for Task Achievement in the Presence of Signal-dependent Noise

Rieko Osu[1], Naoki Kamimura[2], Hiroshi Iwasaki[2], Eri Nakano[3],

Chris M. Harris[4], Yasuhiro Wada[2], and Mitsuo Kawato[1]

1. ATR Computational Neuroscience Laboratories, Kyoto, 619-0288, Japan
2. Nagaoka University of Technology, Niigata, 940-2188, Japan
3. ATR Human Information Processing Research Laboratories, Kyoto, 619-0288, Japan
4. Institute of Neuroscience, University of Plymouth, Plymouth PL4 8AA, U.K.

Abbreviated title (38/60): Optimal Impedance Control with TOPS-α

Corresponding Author

Mitsuo Kawato

ATR Computational Neuroscience Laboratories

2-2-2 Hikaridai, Seika-cho, Soraku-gun

Kyoto, 619-0288 Japan

email: kawato@atr.jp

TEL: +81-774-95-1058

FAX: +81-774-95-2647

Key Words

Impedance control, stiffness, signal-dependent noise, end-point accuracy, single-joint movement, variability, TOPS-α model.

Abstract (243) There is an infinity of impedance parameter values, and thus different co-contraction levels, that can produce similar movement kinematics, from which the central nervous system must select one. Although signal-dependent noise (SDN) predicts larger motor-command variability during higher co-contraction, the relationship between impedance and task performance is not theoretically obvious and thus examined here. Subjects made goal-directed, single-joint elbow movements to either move naturally to different target sizes or voluntarily co-contract at different levels. Stiffness was estimated as the weighted summation of rectified EMG signals through the index of muscle co-contraction around the joint (IMCJ) proposed by Osu et al. (2002). When subjects made movements to targets of different sizes, IMCJ increased with the accuracy requirements, leading to reduced end-point deviations. Therefore, without the need for great accuracy, subjects accepted worse performance with lower co-contraction. When subjects were asked to increase co-contraction, the variability of electromyography (EMG) and torque both increased, suggesting that noise in the neuromotor command increased with muscle activation. In contrast, the final positional error was smallest for the highest IMCJ level. Although co-contraction increases the motor-command noise, the effect of this noise on the task performance is reduced. Subjects were able to regulate their impedance and control end-point variance as the task requirements changed, and they did not voluntarily select the high impedance that generated the minimum end-point error. These data contradict predictions of the SDN-based theory, which postulates minimization of only end-point variance, and thus require its revision.

INTRODUCTION

The central nervous system (CNS) can control the mechanical impedance (inertia, viscosity, and stiffness) of its motor apparatus (Hogan, 1985; McIntyre et al., 1996). For example, viscosity and stiffness can be adjusted through mechanisms such as the co-contraction of muscles. Several studies have examined impedance changes in response to external perturbations. When trying to keep a hand position constant (Mussa-Ivaldi et al., 1984) or moving (Milner and Cloutier, 1993; Burdet et al., 2001) against external perturbing forces, limb stiffness increases. Precise timed increases in stiffness also occur in anticipation of predictable external events, such as catching a ball (Lacquaniti et al., 1993). Impedance changes can also parallel the learning of novel tasks. Milner and Cloutier (1993), Osu et al. (2002, 2003) and Franklin et al. (2003) reported that a co-activation of flexors and extensors is observed in the early stages of dynamic and kinematic learning, with co-activation decreasing with learning. Laursen et al. (1998) and Gribble et al. (2003) found that muscle co-contraction estimated as electromyographic (EMG) activity increased with the higher accuracy requirements of multi-joint arm movements. However, these previous studies did not examine the variability in EMG activity, torque or position dependence on task conditions such as stiffness or accuracy. Furthermore they did not address the effects of volitional impedance changes on attained movement variability or accuracy. Consequently, it is unclear why a particular set of impedance parameters is chosen for a given task from the infinite set of possible impedances that could produce the same endpoint kinematics and forces.

A similar problem has been investigated for the kinematics of movement. Given a reaching task, an infinite number of hand paths and velocities can reach the goal. One framework for selecting a trajectory is optimal control, in which the solution with the smallest cost is selected. Several cost functions (Flash and Hogan, 1985; Uno et al., 1989; Nakano et al., 1999; Wada et al., 2001) have tried to account for the data, but these models are incapable of predicting a trajectory that takes into account the variance that changes according to the changes in motor commands and/or impedance. Since the minimum-jerk model is kinematic, there is no place for impedance. Similarly, the minimum-torque-change model considers joint torque but not muscle tension, so it cannot incorporate impedance within its framework. The minimum-motor-command-change model can actually deal with impedance because it models the motor command for each muscle but always predicts the minimum motor command, thus minimum impedance, which is at odds with the idea of different co-activation levels dependent on different accuracy requirements (Laursen et al., 1998; Gribble et al., 2003). These models neither have variance as a penalty term nor implement noise in motor commands but only deal with a mean or desired trajectory. A recent computational model of movement planning considering the presence of signal dependent noise (Task Optimization in the Presence of Signal-dependent noise: TOPS) may provide a unifying framework that could potentially account for both the kinematics and impedance of a movement. In this framework, the motor commands are assumed to be corrupted by noise, whose standard deviation increases with the level of the motor command (Harris and Wolpert, 1998; Jones et al., 2002). Such signal-dependent noise

(SDN) plays through the muscle dynamics and limb impedance, leading to variability in movement. Different motor commands should thus lead to different movement statistics. The TOPS model proposes that the cost depends on these statistics (Miyamoto et al., 2002; Hamilton and Wolpert, 2002). The motor command is selected to minimize the cost, thus minimizing the deleterious effects of SDN on task performance.

As the SDN plays through the impedance of the limb, the impedance can be changed to modify the consequences of the noise. Similarly, the change in impedance alters the noise in the system because the co-contraction of muscles leads to larger muscle activities, resulting in a larger SDN. Assuming the presence of SDN, impedance should have complicated effects of both increasing and decreasing the movement accuracy. Given that changing either the motor command or impedance can affect the movement statistics, the TOPS model has a potential capability to coherently explain both trajectory planning and impedance control by including impedance parameters within its framework. Therefore, the first aim of this study is to experimentally examine the effects of increased impedance on movement accuracy.

The principle of the TOPS model is that the objective of motor planning is to optimize task statistics in order to increase accuracy (cf. minimizing end-point variance in Harris and Wolpert, 1998). If this principle holds, we expect the optimal impedance for minimizing movement error to be selected in voluntarily executed movements. Then, if subjects are required to specifically increase impedance during movements, a decrease in accuracy is predicted because non-optimal impedance should generate poorer task statistics. On the contrary, if higher movement accuracy is required, subjects should

utilize the same impedance as in ordinary conditions, where impedance is already optimized to maximize accuracy. The second aim of this paper is to examine whether these predictions can be experimentally confirmed.

To investigate the relationship between impedance and movement variability, we examined two tasks. In the first task (target size), accuracy constraints were varied and movement variability and impedance were estimated. In the second task (voluntary co-contraction), impedance was voluntarily controlled and movement variability and accuracy were examined. From the results of these two experiments, we found that impedance does have the above mentioned complicated effects of both increasing SDN and decreasing end-point accuracy and that the data contradicted the predictions made by the TOPS model.

MATERIALS AND METHODS

Thirteen male subjects, aged 20-29 years, participated in at least one of the two experiments, and 11 of them were naïve as to the purpose of the study. Nine subjects participated in the target-size experiment and nine subjects participated in the voluntary co-contraction experiment. For the five subjects who participated in both experiments, the target-size experiment was first carried out and then the voluntary co-contraction experiment was conducted on another day. Each experiment took several hours, since it consisted of EMG electrode attachment, isometric force generation for parameter calibration of IMCJ, preparatory trials to select movement times specific to individual subjects, and main trials. Accordingly, a one- to two-hour lunch break and frequent short rests were allowed. We did not try to estimate muscle viscosity in this study. However, from previous studies (Gomi and Osu, 1998; Osu and Gomi, 1999), we expected that muscle viscosity would co-vary with muscle torque, muscle stiffness, and EMG activity. The Institutional Ethics Committee approved the experiments, and subjects gave informed consent prior to participation.

Experimental apparatus

Subjects sat on a chair and rested their right elbow on a sponge fixed to a table (Fig. 1A). The table was adjusted to lift the subject's arm to shoulder level so that movements were made in a horizontal plane. The upper arm movement was constrained by fixing the shoulder position with a harness and the elbow position with the sponge. The subject's

wrist was braced. To reduce friction between arm and table, the arm was attached to a board that levitated above the table by an air sled (Fig. 1A). Subjects were asked to move only their elbow joint. An OPTOTRAK 3020 was used to measure the position of a marker placed on the end of a 9-cm vertical bar, which was grasped by the subjects. The marker position was sampled at 500 Hz and projected as a cross on a CRT screen, placed in front of the subject, representing current hand position (Figs. 1B and C). Subjects performed the task while looking only at the CRT screen.

Electromyography

Surface EMG activity was recorded using pairs of silver-silver chloride surface electrodes. The activities of two elbow muscles, the brachioradialis and the medial head of the triceps brachii, and two biarticular muscles, the biceps brachii and the long head of the triceps, were recorded. The EMG signals were analog filtered at 25 Hz (high pass) and 1.0 kHz (low pass) with a Nihon Kohden amplifier (MME-3132) and then sampled at 2.0 kHz. All EMG comparisons between different conditions as well as the calibration of IMCJ involved data that were recorded on the same day without removing the electrodes. From a previous study using the same methods (Osu et al., 2002), we confirmed the stationarity of the EMG electrodes by comparing torque-EMG relationships before and after the main experiment.

Stiffness estimation by IMCJ

Gomi and Kawato (1996) and Burdet et al. (2000, 2001) measured stiffness during

multijoint arm movements by applying mechanical perturbations with a robotic manipulandum. Previous studies suggested linear relationships among stiffness, torque, and surface EMG activity signals (Tsuji et al., 1995; Osu and Gomi, 1999). Based on these previous studies, Osu et al. (2002) proposed an index of muscle co-contraction around the joint (IMCJ) to evaluate joint viscoelasticity during movements. IMCJ was defined as the summation of absolute values of antagonistic muscle torques around the joint, and it was computed from the linear relation between surface EMG activity and joint torque. Osu et al. (2002) confirmed that IMCJ during isometric contraction, as well as during movement, correlated well with joint stiffness estimated by the conventional method, i.e., applying mechanical perturbations, and proposed a formula to estimate stiffness from EMG activity through the IMCJ. In this paper, based on Osu et al.'s (2002) method, stiffness during movement was computed for the elbow joint in each trial. Assuming that surface EMG activity is proportional to muscle tension, elbow torque τ can be expressed as follows:

$$\tau = a_1 u_1 - a_2 u_2 + a_3 u_3 - a_4 u_4. \qquad (1)$$

Here, u_1 and u_2 denote surface EMG activity of the elbow flexor and extensor, and u_3 and u_4 denote surface EMG activity of the biarticular flexor and extensor. The parameters a_i include both the moment arm and conversion factor from the muscle activity to muscle tension. Using the parameters a_i, the IMCJ of the elbow is computed as follows:

$$IMCJ = a_1 u_1 + a_2 u_2 + a_3 u_3 + a_4 u_4. \qquad (2)$$

On each day of the experiment and before the main experiment, subjects were asked to

generate six different isometric force temporal patterns with three different levels of force magnitude (maximum forces of 5, 10 and 15 N) with five repetitions (90 trials = 6 x 3 x 5). The force temporal patterns were: i) extend and keep, ii) extend-flex-relax, and iii) extend-relax-extend-relax-extend, with the same three patterns for flexion, all executed within three seconds. The torques and EMG activity recorded in these calibration experiments were used to estimate the parameters a_i of the IMCJ by the least-square-error method (Osu et al., 2002).

We note that the estimation of stiffness from IMCJ should not be taken as a rigorous method. We well realize the existence of variable moment arms during movements, nonlinear properties of muscle tension dependent on muscle length, shortening velocity, and motor commands, all of which work against simple linear models such as IMCJ to estimate the stiffness from EMG activity. However, quantitatively speaking, IMCJ was found to be a good first approximation of stiffness even during movement, which was then independently measured by mechanical perturbations (Osu et al., 2002). At the very least, IMCJ is a much superior and more systematic way of weighting EMG activity from multiple muscles while estimating stiffness than any arbitrary method of weighting (cf. Gribble et al., 2003). In order to demonstrate the robustness of the obtained results for the weighting of EMG activity from multiple muscles, we analyzed identical data using the following two different weighting methods. One is to normalize each muscle's EMG activity by its maximum value, which is the conventional normalization technique but does not lead to a stiffness estimate. The second method is to apply the smooth temporal filter from EMG activity to muscle tension proposed by Koike and Kawato (1995) to data

from both calibration and main experiments to represent the known electro-mechanical delay in computing IMCJ. All three methods of weighting EMG activity led to identical statistical results, and thus only the results obtained by IMCJ without filtering are reported here.

Furthermore, we note that hand paths were almost identical across trials and subjects because only elbow rotation was included, and the joint torques that were generated were also very severely controlled to be the same because the movement duration was experimentally controlled. With these stringent experimental paradigms, we expect that any change in EMG activity is mainly due to a change in co-contraction and stiffness, and not to changes in movement trajectory, velocity, or torque profiles. This at least validates the usage of IMCJ as a "relative" index for stiffness.

To confirm impedance changes in a more primitive way, we compared root-mean-square (RMS) EMG of each muscle. Assuming that EMG and stiffness have a monotonic relation, if the EMGs of all muscles are larger in a particular condition than in other conditions, we can conclude that stiffness was larger in that condition. The RMS EMG was computed during the latter half of the movement, that is, 250 ms before the end of the movement to the end of the movement defined by an acceleration threshold (see below).

Task

The task was a single-joint extension or flexion movement of the elbow, and it followed the experimental paradigm of Gottlieb et al. (1989). In the target-size

experiment, subjects were asked to move their hand from a start circle with a radius of 1.0 cm and enter a target circle with a different radius displayed on a CRT within a desired movement duration (Fig. 1B). In the voluntary co-contraction experiment, subjects were asked to move their hand from a start circle with a radius of 1.0 cm and come as close as possible to a small target point (3-mm radius) displayed on the CRT within a desired movement duration (Fig. 1C). The shoulder angle (θ_1) was fixed to 94 degrees. The start and target positions were either an elbow angle (θ_2) of 41 degrees or 97 degrees, depending on whether the movement was extension or flexion (Fig. 1A). Extension movements were first conducted in a batch, and then flexion movements were carried out. The out-and-in movement duration was defined as the time (sec) between when the hand exited the start circle and entered the target circle and was used throughout the experimental task control. Following the isometric force generation, subjects conducted flexion and extension movements of 20 trials each (preparatory experiment). Because this preparatory experiment was conducted, we did not observe any apparent learning effects in the main experiments. The desired out-and-in movement duration was predetermined by its average over the last ten trials during the preparatory experiment to make the movement duration comfortable for each subject. The desired out-and-in movement durations ranged between 0.232 and 0.325 (sec) for all subjects in the target-size experiment and between 0.250 and 0.334 (sec) in the voluntary co-contraction experiment. For each subject, only movements with an allowable error of ±10% of the pre-specified out-and-in desired movement duration were recorded as successful movements. A computer program checked whether the movement duration was within

the allowable range, and a warning of ‘too early,’ ‘too late,’ or ‘out of target’ was fed back to the subjects after each trial when the hand entered the target circle too soon, too late, or did not end within the target circle, respectively. For the target-size experiment, average success rates and standard deviations across subjects for large, medium, and small targets were 70±14%, 62±14%, and 45±13% respectively. For the voluntary co-contraction experiment, average success rates and standard deviations across subjects for normal, medium, and high co-contraction were 58±20%, 66±11%, and 62±25% respectively.

Experiment I: Changed target size

The task was to move (flex or extend) the hand to different-sized target circles. The radii of the target circles were 3.5 cm, 2.5 cm, and 1.5 cm for large, medium, and small conditions, and they were presented in this order to subjects. Subjects were requested to bring their hand within a target at the end of the movement. We recorded 40 successful trials in which the hand reached the target within the allowable time range for each target size and for either flexion or extension; 240 successful trials (2 directions x 3 sizes x 40 trials) were recorded and used for analysis. The desired out-and-in movement duration was corrected for the different distances that were traveled to the different target sizes. No instructions were given on co-contraction. Although EMG signals were recorded, muscle activity was not fed back to the subjects (Fig. 1B).

Experiment II: Changed co-contraction level

The task was to execute extension or flexion movement under three levels of muscle

co-contraction: a normal level with elbow muscles relaxed; a high level in which elbow muscles were strongly co-contracted so that the arm became stiff; and a medium level of co-contraction between normal and high. In order to avoid presentation of the target region that explicitly instructs the permitted end-point variability, a small target point was presented instead of a target circle. The subjects moved their hand from a start circle to as close as possible to the target point. The out-and-in movement duration was measured as the time interval between when the hand exited the start circle and entered a virtual end-point-domain circle with a radius of 5 cm, whose range was shown by two tangent lines on the CRT (Fig. 1C).

In the medium and high levels, subjects had to voluntarily co-activate their muscles during movements. Because the strength of muscles varies between subjects, the activation levels were set before the main experiment in preparatory trials. In this phase, 20 trials each for the normal and high conditions, in which the arm was relaxed or stiffened, and for both flexion and extension, were preliminarily recorded when the hand reached the virtual end-point-domain circle within the time limit. The elbow stiffness in 80 movement trials (2 co-contraction conditions x 2 directions x 20 trials) was estimated by IMCJ. For each subject, the observed IMCJ range was divided into high, medium and low ranges. For each trial in the main experiment, elbow IMCJ was computed to determine whether it was within the predetermined range of the corresponding co-contraction condition. The success or failure of achieving this required IMCJ level was fed back to the subject at the end of each trial. To help subjects set an appropriate co-contraction, the recorded EMG signals were shown on the CRT in real time to the

subjects from before the start of movement (Fig. 1C). We recorded 40 successful trials for each level of co-contraction and for each direction of flexion and extension. Altogether, 240 successful trials were obtained (3 stiffness conditions x 2 directions x 40 trials). The order of the three co-contraction conditions was counterbalanced across subjects.

Analysis

Position data were digitally filtered by a third-order Butterworth filter with an upper cutoff frequency of 15 Hz. Derivatives of the position data were computed by applying a three-point local polynomial approximation. The start and end points of each movement were determined using an angular acceleration with a 1.0 rad/s^2 threshold. The movement duration determined from these start and end points was called kinematic movement duration, and it was nearly two times longer than the out-and-in movement duration. The out-and-in movement duration was used only to control the movement duration during the main experiment, and the kinematic movement duration was used for all data analyses. The averages of kinematic movement durations for the three target sizes and for individual subjects were within the range of 0.462–0.533 sec, and those for the voluntary co-contraction experiment were within 0.520–0.616 sec. The actuated torque of the elbow τ was calculated as the product of the estimated inertial moment of the forearm from each subject's body size and the angular acceleration of the elbow joint. We did not include a viscosity term in the calculation of the torque because most of the viscosity measured around a joint arises from biochemical and mechanical processes within the muscle rather than from the properties of the joint (Akazawa, 1994). The effect of gravity

was ignored because the arm was supported against gravity by the air sleds to reduce friction.

We examined whether experimental conditions such as target sizes and the level of co-contraction affect EMG activity, torque, position, and end points. Accordingly, we first computed the ensemble-averaged temporal profiles over 40 trials of each signal. Ensemble-averaged rectified EMG activity of the *i*-th muscle at time *t* was as follows:

$$EnsAveE_i(t) = \frac{1}{40}\sum_{j=1}^{40}\left|e_i^j(t)\right| \qquad (3)$$

where $e_i^j(t)$ denotes EMG activity of the *i*-th muscle at time *t* of the *j*-th trial. Ensemble-averaged torque at time *t* was

$$EnsAveT(t) = \frac{1}{40}\sum_{j=1}^{40}\tau^j(t) \qquad (4)$$

where $\tau^j(t)$ denotes torque at time *t* of the *j*-th trial. Similarly, ensemble-averaged *x*-position and *y*-position were computed as follows:

$$EnsAveP_x(t) = \frac{1}{40}\sum_{j=1}^{40}x^j(t) \qquad (5)$$

$$EnsAveP_y(t) = \frac{1}{40}\sum_{j=1}^{40}y^j(t) \qquad (6)$$

where $x^j(t)$ and $y^j(t)$ denote *x*-position and *y*-position at time *t* of the *j*-th trial. Signals are aligned so that the first 1.0 rad/s^2 absolute angular acceleration threshold of ballistic movements determines time zero. Movement duration for each signal was normalized within the same experimental condition to mean movement duration of that condition, without changing the amplitude of the signal (see below for detail). The ensemble-averaged temporal waveforms of IMCJ and velocity profiles were computed in

the same way. These allow the deviation time course of each trial to be calculated as the difference from the ensemble-averaged time courses. The ensemble-averaged deviation is defined as the root mean square of this deviation time course over 40 trials. Therefore, ensemble-averaged deviation of rectified EMG of the *i*-th muscle and ensemble-averaged deviation of torque at time *t* are computed as follows:

$$EnsDevE_i(t) = \left[\frac{1}{40} \sum_{j=1}^{40} \left(EnsAveE_i(t) - \left| e_i^j(t) \right| \right)^2 \right]^{0.5} \quad (7)$$

$$EnsDevT(t) = \left[\frac{1}{40} \sum_{j=1}^{40} \left(EnsAveT(t) - \tau^j(t) \right)^2 \right]^{0.5} \quad (8)$$

In other words, we studied the variability across trials at each point in time. As already mentioned in the description of stiffness estimation by IMCJ, we examined the effect of first smoothing the EMG signal by the temporal filter of Koike et al. (1995), and the same results were obtained regarding the relation between EMG amplitude and variance. Finally, we computed the time-averaged magnitude and deviation on a per trial basis. The time-averaged EMG of the *j*-th trial was computed as mean rectified EMG between the time at the beginning and the time at the end of movement t_f, summed over all muscles.

$$TimeAveE_j = \sum_{i=1}^{4} \frac{1}{t_f} \sum_{t=1}^{t_f} \left| e_i^j(t) \right| \quad (9)$$

The time averaged IMCJ magnitude of the *j*-th trial was computed in the same way:

$$TimeAveIMCJ_j = \frac{1}{t_f} \sum_{t=1}^{t_f} IMCJ^j(t) \quad (10)$$

The time-averaged deviation of the *j*-th trial was computed as the square root of the mean squared deviation time course between the time at the beginning and the time at the end of

movement t_f:

$$TimeDevE_j = \left[\sum_{i=1}^{4} \frac{1}{t_f} \sum_{t=1}^{t_f} \left(EnsAveE_i(t) - \left| e_i^j(t) \right| \right)^2 \right]^{0.5} \quad (11)$$

$$TimeDevT_j = \left[\frac{1}{t_f} \sum_{t=1}^{t_f} \left(EnsAveT(t) - \tau^j(t) \right)^2 \right]^{0.5} \quad (12)$$

$$TimeAveP_j = \left[\frac{1}{t_f} \sum_{t=1}^{t_f} \left\{ \left(EnsAveP_x(t) - x(t) \right)^2 - \left(EnsAveP_y(t) - y(t) \right)^2 \right\} \right]^{0.5} \quad (13)$$

The amount of scatter at end-points, that is, end-point deviation, was indicated by the standard deviation of end-point positions. On the other hand, the end-point error was defined as the root mean square of the distance between the end-point positions and the center of the small target point. End-point deviation and end-point error are generally different because the average end-point position deviates from the target center (Gribble et al., 2003). Also, end-point error is not an appropriate terminology for an analysis of the target-size experiment because subjects were not required to reach for the centers of target circles, and movements ending within target circles were regarded as successful. To examine the effect of SDN to various level of movement variance on a trial-by-trial basis, we investigated the correlation between the time-averaged IMCJ of an individual trial (Eq. 10) and the time-averaged deviations of the torque (Eq. 12), position (Eq. 13), and end-point of the hand in that trial. In addition, we investigated the correlation between the time-averaged EMG activity (Eq. 9) and the time-averaged EMG deviation (Eq. 11). The correlation coefficients obtained from these trial-by-trial analyses are shown in Fig. 11. To investigate SDN during movements, we computed correlation coefficients and slopes

for liner relationships between ensemble-averaged EMG (Eq. 3) and ensemble-averaged EMG deviation (Eq. 7) at each time point for each muscle of each subject.

In the computations of ensemble-averaged temporal waveforms and time-averaged deviations of position and torque, the time was normalized within the same experimental conditions to mean movement time of that condition. That is, for each trial, each value (position, velocity and torque) was first computed, where the movement beginning and end was defined by the acceleration threshold, as explained above. Then each value was scaled only in time domain to mean movement time of each condition by re-sampling using spline interpolation. Therefore, the normalization did not change the amplitude of each signal. We also adopted two other methods of ensemble averaging without time normalization. In both methods, the physical time was used in ensemble averaging over 40 trials, and all data in one condition were first aligned at the time of movement start. In the second method, all data in one condition were cut at the time of the termination of the movement whose duration was shortest in that condition. In the third method, all data in one condition were cut at the time of the termination of the movement whose duration was longest in that condition, and then the values between the termination of each movement and the time of data cutting were fixed to the value at the end of each movement to avoid distortion due to feedback correction or oscillation. Here, we show the results using the first method because the results obtained from all three methods are similar.

In order to examine the effect of the target-size or muscle co-contraction levels on mean performance, we carried out a 2-way repeated measures analysis of variance

(repeated measure ANOVA, target-size or co-contraction levels x movement directions), with subjects as a random factor, for time-averaged IMCJ, time-averaged deviations of EMG activity, torque and position, and end-point as well as end-point errors and RMS EMG using data for all subjects. F-ratios were computed by treating the target size or co-contraction levels and movement directions as within-subject factors. This was followed by Tukey's HSD test.

RESULTS

Signal-dependent noise during movements

In order to examine signal dependent noise during movements, we computed signal magnitude and its deviation at each time point of movements. Because EMG signals during movements are not stationary, time courses of EMG magnitude were computed as an ensemble average of rectified EMG time course over 40 trials (Eq. 3). Then, time courses of EMG deviations were computed as the root mean square of difference between each one and the ensemble-averaged EMG time course over 40 trials (Eq. 7). Then, EMG deviation at each time point was plotted against EMG magnitude at that time point for each muscle and each movement direction, for each condition of each experiment, and for each subject. Figure 2 shows plots of a typical subject during a voluntary co-contraction experiment. Blue, red, and green dots denote normal, medium, and high co-contraction conditions, respectively. In all comparisons, EMG deviation linearly increased with EMG magnitude. The mean and standard deviation of correlation coefficients across muscles, subjects and conditions were 0.843±0.092 for extension and 0,821±0.099 for flexion in the target-size experiment, and 0.814±0.087 for extension and 0.814±0.088 for flexion in the voluntary co-contraction experiment. We also computed slopes between EMG mean and deviation for each comparison. Figure 3 shows the histogram of the slopes for each movement direction. The slopes widely raged from around 0.5 to 3 with a mean of 1.192±0.422, which include the predicted slopes of uniform, Gaussian, and Laplacian

distribution (0.58, 0.76, and 1.00, respectively) within the 2SD region, suggesting that the observed linear relationship is not a trivial mathematical result (see Discussion for detail). The slopes were significantly larger when muscles were working as antagonists than as agonists for both target size (*t*-test, $t(214) = 4.72$; $P < 0.0001$) and voluntary co-contraction experiment ($t(214) = 3.60$; $P < 0.0005$).

Experiment I: Changed target size

The averages and standard deviations of the kinematic movement durations across subjects for the large, medium and small target sizes were 0.498±0.069, 0.497±0.069, and 0.491±0.062 sec, respectively, and were not significantly different. Figure 4 shows the hand paths, end-point distributions (A), angular velocity profiles (B), torque profiles (C), EMG time courses of the four muscles (D), and stiffness profiles (E) of a typical subject recorded for the different target sizes for extension movements. These characteristics are in good agreement with previous studies (Gottlieb et al., 1989). The end-points of the hand were distributed along an arc within target circles (Fig. 4A). Therefore, the end-point deviation increased as the target size increased in accordance with our experimental design (see below and Fig. 7F). The angular velocity profiles were bell-shaped, and corrective movements were not observed. Although the hand paths (A), velocity (B), and torque profiles (C) were similar for the three different target sizes, co-activation of bi-articulator muscles (D) and resulting IMCJ increase (E) were evident in the latter half of movement for the more stringent accuracy requirements.

Figure 5 shows the ensemble-averaged time courses across all subjects and all trials

classified by target size for the summed EMG activity over the four muscles (A) (Eq. 3), IMCJ (B), torque (C) (Eq. 4), and velocity (D), as well as the ensemble-averaged deviations across all subjects for the summed EMG activity (E) (Eq. 7; summed over the four muscles before taking square root), torque (F) (Eq. 8), and position (G). The data from extension (upper panel) and flexion (lower panel) are shown separately. Blue, red, and green indicate large, medium, and small target sizes, respectively. While average time courses for torque (C) and velocity (D) were similar for different target sizes for both extension and flexion, the summed EMG activity (A) and IMCJ (B) profiles of the small target size were larger (green curves; see Figs. 7A and B for statistics), suggesting that co-contraction increased as target size decreased. In good agreement with the assumption of SDN, the EMG deviations were also generally larger for the small target size (Fig. 5E). However, no general or marked differences between different target sizes were observed for the torque and position deviations (Figs. 5F and G), except for the position deviation around movement end as shown in the magnified inset (Fig. 5H), suggesting that noise observed in the motor command was attenuated at torque and position levels. Further, around 0.4 sec after movement onset, three curves representing the positional deviations for the three target sizes came very close in extension and crossed in flexion. Accordingly, after 0.4 sec the positional deviation for the smaller target size was smaller in accordance with the task requirements, despite the large EMG deviation.

To confirm that co-contraction increased later in the movement for higher accuracy requirements, we plotted the late RMS EMG of each muscle for each subject and movement direction against target sizes (Fig. 6). For all four muscles, late RMS EMG for

small target was significantly larger than that for medium and large targets (repeated measures ANOVA; see figure legend and insets for statistics). This suggests that co-contraction was utilized to control end-point accuracy.

Figure 7 shows observations similar to those shown in Fig. 5 and their statistics in time-averaged data. Figs. 7A and B again demonstrate an increased motor command with a decreased target size. Figure 7A shows the means and standard deviations across all subjects for each target size of the summed EMG activity that was time-averaged over the entire movement duration. Figure 7B shows those for the time-averaged IMCJ. The gray lines denote extension and the black lines denote flexion data. The horizontal lines in Fig. 7 indicate significant comparisons in post-hoc tests ($p < 0.05$). The main effect of the target size was significant for the amount of muscle activity in terms of the time-averaged summed EMG activity ($F(2,16) = 10.86$; $P < 0.005$) (Fig. 7A) as well as the time-averaged IMCJ ($F(2,16) = 12.22$; $P < 0.001$) (Fig. 7B). The muscle co-contraction, examined either as the time-averaged summed EMG activity or the time-averaged elbow IMCJ, was significantly higher in the small target than the medium and large targets for both flexion and extension. Other figures demonstrate that target size has a different effect on different deviations. Figs. 7C, D, and E show the means and standard deviations across subjects for each target size of the deviations that were time-averaged over the entire movement duration for EMG activity, torque, and position, respectively (see Methods for equations of time-averaged deviations). Figure 7F shows the mean and standard deviation of the end-point deviation across subjects for each target size. The main effect of the target size was significant for the time-averaged deviation of EMG

activity ($F(2,16) = 12.27$; $P < 0.001$), and the end-point deviation ($F(2,16) = 157.80$; $P < 0.0001$). The EMG variability was significantly largest for the small targets both for extension and flexion, which is consistent with SDN. In contrast, the end-point deviation was significantly larger in the large target than the medium target and significantly larger in the medium target than the small target; consequently, the experimental manipulation of the end-point variability went well for the target-size experiment.

Similar trends to Figs. 5 and 7 were observed when EMG activity, torque, and position ensemble averages and deviations were calculated using the shortest movement duration of each condition (the second method; see MATERIALS AND METHODS) or when using duration of each movement and extrapolate by the final value until longest movement duration (the third method; see MATERIALS AND METHODS). The summed EMG activity ($F(2,16) = 8.35$; $P < 0.005$ for shortest movement duration, $F(2,16) = 11.90$; $P < 0.001$ for longest movement duration) and IMCJ ($F(2,16) = 9.12$; $P < 0.005$ for shortest movement duration, $F(2,16) = 11.85$; $P < 0.001$ for longest movement duration) were significantly different and were largest for the small targets.

Experiment II: Changed muscle activation level

The means and standard deviations of the kinematic movement durations across subjects for the normal, medium and high co-contraction conditions were 0.581±0.073, 0.558±0.071, and 0.537±0.062 sec, respectively, and decreased significantly for the higher co-contraction level, although the predetermined desired out-and-in movement duration was the same for the three conditions. Figure 8 shows the hand paths, end-point

positions, angular velocity profiles, torque profiles, EMG time courses of the four muscles, and IMCJ profiles recorded for the three levels of co-contraction for the same subject, in a similar format to Fig. 4. The end-points of the hand were distributed along an arc around the target point more narrowly for the larger co-contraction level (Fig. 8A). The angular velocity profiles were bell-shaped, and corrective movements were not observed. Although the EMG activity of all four muscles (Fig. 8D) and IMCJ (Fig. 8E) were much larger over the entire movement duration for the higher level of co-contraction, the ensemble-averaged hand paths (Fig. 8A), velocity (Fig. 8B), and torque profiles (Fig. 8C) were similar among the three co-contraction conditions. However, we must note that the velocity profiles for high co-contraction were more symmetrical than those for low co-contraction (Figs. 8B and 9D). The velocity peak in low co-contraction condition was slightly, but significantly earlier than in medium and high co-contraction conditions ($F(2,16) = 20.50$; $P < 0.0001$). Mean velocity peak in low co-contraction condition was significantly earlier than the mid point of movement duration (*t*-test, $t(8) = 2.67$; $P < 0.05$ for extension, $t(8) = 3.41$; $P < 0.01$ for flexion) while that in high co-contraction condition was not significantly different ($t(8) = 1.05$; $P = 0.32$ for extension, $t(8) = 1.83$; $P = 0.10$ for flexion), suggesting that velocity profiles for high co-contraction condition were significantly more symmetrical.

Figure 9 shows the ensemble-averaged time courses of the summed EMG activity, IMCJ, torque, and velocity as well as the ensemble-averaged deviation time courses of the summed EMG activity, torque, and position classified by co-contraction levels combining data from all subjects and all trials, in a similar format to Fig. 5. Blue, red, and

green indicate normal, medium, and high co-contraction conditions, respectively. While the average time courses for the torque and velocity were similar for different co-contraction levels (Figs. 9C and D), the summed EMG activity and IMCJ profiles for the larger co-contraction conditions were larger (Figs. 9A and B), which shows that subjects actually followed the instruction and could voluntary control co-contraction levels. In good agreement with SDN assumption, the time courses of EMG activity, torque, and position deviations were generally larger for the larger co-contraction conditions (Figs. 9E, F and G), except for the position deviation around movement end as shown in the magnified inset (Fig. 9H). Around 0.5 sec after the movement onset, however, three curves representing the positional deviation for the three co-contraction levels converged and/or crossed. That is, after 0.5 sec, the positional deviation for the different co-contraction levels became nearly indistinguishable, suggesting attenuation of SDN. Data from extension and flexion were qualitatively similar.

Figure 10 shows observations similar to those shown in Fig. 9 and their statistics in time-averaged data. Figs. 10A and B show the mean and standard deviation across all subjects of the time-averaged summed EMG activity and time-averaged IMCJ, respectively, for each co-activation requirement. The gray lines denote extension, and the black lines denote flexion. The horizontal lines indicate significant comparisons in post-hoc tests ($P < 0.05$). The main effect of the muscle co-activation requirement was significant for the amount of muscle activity in terms of time-averaged summed EMG activity ($F(2,16) = 29.09$; $P < 0.0001$) as well as time-averaged IMCJ ($F(2,16) = 17.16$; $P < 0.0005$). Furthermore, the muscle activity, that is, arm IMCJ, was significantly smallest

in the normal level and significantly largest in the high level. Accordingly, the main task design of the voluntary co-contraction experiment was fulfilled. Other figures demonstrate that the co-activation level has different effect on different deviations. Figs. 10C, D, and E show the mean and standard deviations across all subjects for time-averaged deviations of EMG activity, torque, and position, respectively, for each co-contraction requirement. Figs. 10F and G show the mean and standard deviations across all subjects for the position deviation at the end point as well as the end-point error for each co-contraction requirement. A larger variability in EMG activity, torque, and position was observed for the higher muscle activation level, although there was no such trend for the end-point deviation, and the relationship was reversed for the end-point error. The main effects of the muscle activation level were significant for variabilities in EMG activity ($F(2,16) = 40.04$; $P < 0.0001$), torque ($F(2,16) = 66.53$; $P < 0.0001$), position ($F(2,16) = 11.74$; $P < 0.001$), and end-point error ($F(2,16) = 6.26$; $P < 0.01$). The variabilities in EMG activity and torque were significantly larger in the high level and smaller in the normal level. The end-point error in the normal level was significantly larger than in the medium and high levels for both extension and flexion.

The same trends shown in Figs. 9 and 10 were observed when the EMG activity, torque and position deviations were calculated using the shortest movement duration of each condition (the second method; see MATERIALS AND METHODS) or when using the duration of each movement and extrapolating by the final value until the longest movement duration (the third method; see MATERIALS AND METHODS). That is, these variabilities were significantly different (EMG deviation; $F(2,16) = 28.59$; $P <$

0.0001 for shortest duration, $F(2,16) = 30.45$; $P < 0.0001$ for longest duration, torque deviation; $F(2,16) = 32.19$; $P < 0.0001$ for shortest duration, $F(2,16) = 30.78$; $P < 0.0001$ for longest duration, position deviation; $F(2,16) = 10.10$; $P < 0.005$ for shortest duration, $F(2,16) = 8.84$; $P < 0.005$ for longest duration) and larger at the high level but smaller at the normal level.

The observed reversed relationship between motor command magnitude and end-point error suggests that SDN is attenuated as the space shifts from intrinsic motor command space to extrinsic task space. Noise was highly positively correlated with magnitude of motor command at EMG or torque level but was negatively correlated at target achievement level. To further demonstrate the degradation of correlation between motor command magnitude and deviations, we computed the correlation coefficients between the co-contraction magnitude and EMG deviation, torque deviation, position deviation, end-point deviation, and end-point error on a trial-by-trial basis (Figure 11). For each movement trial of an individual subject, such as those shown in Fig. 8, the following seven quantities were first computed. The first two were the summed rectified EMG activity and its deviation, both of which were time-averaged over movement duration. The equations are given in Materials and Methods (Eqs. 9 and 11). The third to fifth were IMCJ and the deviations of torque and position, all of which were time-averaged over movement duration. The equations are given in Materials and Methods (Eqs. 10, 12, and 13). The last two quantities were end-point deviation and the end-point error. Then, for each subject and for each movement direction, a correlation coefficient was computed from 120 movement trials (40 trials x 3 stiffness conditions)

between two quantities for each of the following five pairs. The first is between the time-averaged summed EMG activity and its time-averaged deviation. The second is between the time-averaged IMCJ and the time-averaged torque deviation. The third is between the time-averaged IMCJ and the time-averaged position deviation. The fourth is between the time-averaged IMCJ and the end-point deviation. The fifth is between the time-averaged IMCJ and the end-point error. Figure 11A plots these 18 correlation coefficients (2 movement directions x 9 subjects) for the voluntary co-contraction experiment while connecting the same subject by the thin line and representing the same movement direction by the same symbol. The light and dark shaded regions show the insignificance ranges of correlation coefficients, outside of which the coefficient is statistically different from zero for an individual data item and the data from all subjects, respectively. For the relationship between EMG activity and EMG variability, the correlation coefficients of all subjects were positive and very close to 1 (Fig. 11A leftmost). The correlation coefficients of IMCJ and torque variability were positive and relatively high and significant for all but one subject (Fig. 11A second from left). The correlation coefficients of IMCJ and position variability were positive for 15 out of 18 cases and relatively small and insignificant for most subjects (Fig. 11A middle). The correlation between IMCJ and end-point deviation was positive or negative depending on the subject and movement direction, and most coefficients were small in magnitude and insignificant (Fig. 11A second from right). The correlation coefficients between IMCJ and end-point error were negative in 13 out of 18 cases and some were significant (Fig. 11A rightmost). Figure 11A also shows, by thick black lines and asterisks, the correlation

coefficients for the five relationships computed from all 2,160 trials of all subjects. The correlation coefficient was close to 1 and significant for EMG deviation. It was positive and significant for torque deviation. It was slightly positive but significant for position deviation. It was slightly negative but significant for end-point deviation, and negative and significant for end-point error. Figure 11B plots the same correlation coefficients for the relationships from the target-size experiment and shows similar trends.

DISCUSSION

We showed that when subjects made single-joint elbow movements to targets of different diameters, IMCJ and EMG variability increased with the required accuracy of the task and reduced end-point variability. When subjects were asked to increase co-contraction during movements, the temporal profiles of EMG activity and torque both increased in variability. However, final positional error was largest for the lowest and normal co-contraction levels. The qualitative trends of EMG activity, torque, and position variabilities and end-point deviations and error with respect to increased IMCJ were similar between these two experiments, although the range of co-contraction in response to different target sizes was over a much smaller range than could be voluntarily elicited (an 11% versus 196% increase). SDN suggests high correlation between motor command magnitude and movement deviation, but this is true only for intrinsic parameters such as EMG and torque. For the parameters in the task space (Cartesian space), the correlations are low and at the final task level (endpoint error); furthermore, correlation was negative, meaning that SDN no longer holds. This demonstrates that SDN is not sufficient to

explain movement variance, but actually SDN is attenuated by impedance at the task level. Such reversed relationship between EMG variability and positional variability has also been observed when movement speed was increased (Darling and Cooke, 1987).

Signal-dependent noise during movement

When subjects were asked to move with larger co-contraction levels, they increased the motor command signals of the flexor and extensor simultaneously. It has been suggested that the standard deviation of the neuromotor commands increases with its mean based on both motoneuronal firing studies (Clamman, 1969; Matthews, 1996) and surface rectified EMG signals (St-Amant et al., 1998; Clancy and Hogan, 1999) during static force tasks. Psychophysical studies of isometric force production have shown a strong relationship between mean force level and force variability as measured by standard deviation (Schmidt et al., 1979; Sherwood and Schmidt, 1980; Sherwood et al., 1988; Jones et al., 2002). Sherwood et al. (1988) also reported a strong relationship between mean force level and force variability in the elbow-joint movement task when different loads were added to a hand-held bar.

These previous behavioral studies investigated the change in force variability in isometric tasks (Schmidt et al., 1979; Sherwood and Schmidt, 1980; Jones et al., 2002) or moving conditions under normal co-contraction (Sherwood et al., 1988). The current study is the first to examine the relationships between stiffness, EMG activity, torque, and position variabilities and end-point deviation and error during movements. Analysis of EMG variability demonstrated a strong linear relationship with the rectified EMG level

(Fig. 2). This is not a trivial mathematical result of rectifying an AC signal. For a stochastic variable x with zero mean and even probability distribution, there is generally no linear relationship between the standard deviation and mean of the rectified signal. If the distribution changes its shape with different motor command levels, not only the linear relationship but also the monotonically increasing relationship of the deviation as a function of mean may not hold. For an evenly distributed zero-mean random variable x, the variance of the rectified signal is given as follows: $V(|x|) = V(x) - E(|x|)^2$. From this, the observed linear relationship holds if and only if $V(x)$ is proportional to $E(|x|)^2$, which is not a generic property of the zero-mean even distribution. This condition is satisfied for well-known uniform, Gaussian and Laplacian distributions, where the predicted slopes are approximately 0.58, 0.76 and 1.00, respectively. That is, if either uniform, Gausssian, or Laplace distribution is maintained for different levels of motor commands, the linear relationship between the mean and the standard deviation is mathematically derived. For our data, the slope between EMG deviation and magnitude widely raged with a mean larger than that of Laplace distribution (Fig. 3), suggesting that the EMG signal is corrupted by larger noise when the mean level of the signal becomes large. Our results also suggest that movement EMG distributions ranged wider than those in a constant-force, constant-angle condition, which fell between Gaussian and Laplacian distributions (Clancy and Hogan, 1999). Furthermore, the deviation is measured as a root mean squared distance from the ensemble-averaged rectified trajectory, showing true variability in the non-stationary signal. This allows EMG variability to be measured *during movement* for the first time. Consequently, signal-dependent noise was confirmed

during single-joint movements.

Negative correlation of end-point error with stiffness

Analysis of torque variability in the voluntary co-contraction experiment (Figs. 10D and 11A) showed that it increased with stiffness but with a weaker correlation than EMG variability. The positional variability averaged over the movement duration also increased significantly with IMCJ, but with an even weaker correlation (Figs. 10E and 11A). In stark contrast, the final end-point error was significantly larger for the lowest co-contraction level than for the medium or high level (Figs. 10G and 11A). For the higher accuracy requirements of the target-size experiment, subjects chose a higher IMCJ level and achieved a lower end-point deviation (Fig. 7). Therefore, subjects exploited the relationship between stiffness and accuracy as the task demands changed.

Although these findings seem counter-intuitive because higher stiffness involves larger motor commands, resulting in larger signal-dependent noise, they can be reconciled within the extended TOPS framework as will be explained later. Co-contraction has two effects within this model. First, it increases the noise produced by the actuators; although some of the forces in co-contraction cancel each other out, the variabilities from both agonist and antagonist are additive. Second, it changes the impedance of the limb. The impedance determines how the noise plays through the motor apparatus into the end-point error. Figure 11 most markedly demonstrates this effect of decreased and reversed correlation with IMCJ as the signal is transformed from EMG activity to torque, to position, to end-point variability, and finally to end-point error.

Decreased end-point error under higher co-contraction might be explained by two control mechanisms. One is the impedance control that utilizes the muscle's intrinsic spring properties to realize a desired trajectory or end point in negative feedback control (Hogan, 1985; Burdet et al., 2001; Osu et al., 2002; Franklin et al., 2003). When muscle stiffness is increased by feedforward and predictive co-contraction, the increased feedback gains bring higher accuracy. The achievement of the desired trajectory and end-point is suggested because the end-point error decreased while the end-point deviation showed no definite trend as IMCJ increased in the co-contraction control experiment (Figs. 10F and G). Furthermore, in the target size experiment, the positional deviation decreased with higher stiffness (small target size) only in the late stage of movement (Fig. 5G), corresponding to the larger EMG activity and IMCJ in only the latter half of movement duration (Figs. 5A and B). A second possible control mechanism is the optimal feedback control proposed by Todorov and Jordan (2002), where time variant feedback gains are optimally selected based on neural feedback computations rather than muscle co-contraction. This computational theory seems to suggest larger torque variability for higher gains of neural feedback loops, which seems at odds with our results showing higher stiffness and accuracy with little change in torque variability (Figs. 7D and F). Therefore, we may conclude that co-contraction leads to a trade-off between increased noise and reduced consequences due to the changed impedance. In our experiment, the increased variability of position seen during movement can be interpreted as the effects of increased SDN, whereas the reduced final error may be due to the

impedance change, which reduces variability.

In the co-contracted state, the limb is clearly more stable against external noise or perturbations. However, because there was no explicit external perturbation in the current experiments it is not appropriate to ascribe the observed reduction of final task error to the rejection of external perturbation. One possible explanation is other uncontrolled internal processes that can have an effect on final accuracy, such as for example an increase in the overall level of attention, were triggered by the increase of co-contraction. That is, accuracy and impedance are independently regulated and subject generated higher levels of co-contraction while producing less variable feedforward commands. Another possible explanation is that at some level of co-contraction the limb may also be more stable against internally generated noise. How the impedance could reduce the internally generated noise is an open question because the reference trajectory, or the equilibrium position itself, could be perturbed by internally generated noise. Assuming that muscle visco-elasticity changes according to muscle activation (Bizzi et al., 1984), the equilibrium position can be expressed as the difference of two antagonistic muscles' activation divided by the summation of their activation (co-contraction), i.e. $(u_{flex} - u_{ext})/(u_{flex} + u_{ext})$ (Hogan, 1984). When noise is added to one or both of the two antagonistic muscles, changes in the equilibrium position generated by the noise are smaller when the denominator, that is, the amount of co-contraction, is larger. Therefore, the effect of internally generated noise on the reference trajectory may possibly smaller when stiffness is larger. Thus, co-contraction could possibly be one of factors in reducing the effect of internally generated noise on the final endpoint variability.

Shorter movement duration with higher stiffness

In the co-contraction control experiment, a significantly shorter kinematic movement duration was observed with larger co-contraction, although the required out-and-in movement duration was constant irrespective of the co-contraction level. In the target-size experiment, the same effect was observed, although it was much smaller and not significant. A shorter movement duration for higher accuracy is apparently contrary to Fitts' law (Fitts, 1954; Hirayama et al., 1993) and to TOPS model, which predicts Fitts' law (Harris and Wolpert, 1998). A shorter movement duration with higher stiffness may be interpreted as a consequence of the mechanical resonant frequency of the forearm link, which increases in proportion to the square root of the elbow stiffness. The shorter movement duration with the same movement amplitude leads to higher acceleration and larger EMG activity, but this effect is negligible compared with large differences in EMG levels. That is, movement duration change was only 1.48% and 7.52%, while stiffness increase was 11% and 196% in the target-size and co-contraction control experiments, respectively. Assuming that EMG linearly increases with muscle torque and stiffness, it is expected that joint torque, and thus the reciprocal component of EMG, change with the square of duration change. Although a higher-order relationship between EMG and duration might exist because of the nonlinearity between EMG and stiffness, the order-of-magnitude smaller change of movement duration compared with IMCJ increase suggests that IMCJ increase was not merely due to reciprocal activation caused by joint torque increase but mainly due to additional co-contraction. The movement trajectories

and torque profiles were very similar between different experimental conditions (see Figs. 5C, D; Figs. 9C, D), and their differences were too small to explain differences in EMG activity and IMCJ changes. Because the kinematic and dynamic features of the movements are almost invariant across different experimental conditions, IMCJ could be regarded at least as a good relative measure for stiffness, as discussed in Materials and Methods. For similar movement trajectory, IMCJ has been demonstrated to linearly increase with stiffness (Osu et al., 2002). Thus, we conclude that the stiffness changes were caused by the different accuracy requirements and voluntary co-contraction.

Stiffness control dependence on tasks

The largest end-point errors were observed when subjects did not increase co-contraction above the normal level. Similarly, subjects could increase their accuracy in response to a smaller target by increasing co-contraction. Consequently, without the need for greater accuracy, subjects accepted worse performance but with lower stiffness. This contradicts the principle of TOPS and suggests that minimizing the end-point deviation or end-point error alone may not be the sole consideration for task optimization. There is an extra dimension to stiffness control, which increases accuracy but also leads to undesirable factors. For example, the CNS may adopt criteria such as minimization of fatigue (Dul et al., 1984), energy consumption (Alexander, 1997), commanded torque change (Nakano et al., 1999), or motor command change (Kawato, 1992) in combination with the maximization of task achievement. Miyamoto et al. (2002), and Nagata et al. (2002) demonstrated that the TOPS-α model, where a cost term in the motor command

magnitude multiplied by α is added to the task achievement term, gives better prediction of trajectories than the TOPS model for a large number of point-to-point movements. The TOPS-α model combines maximization of task achievement and minimization of motor command magnitude. The relative contribution of these two terms to the overall cost is determined by the coefficient α, which is the weighting constant for motor command magnitude. If α is zero, the TOPS-α model is the same as the TOPS model, which maximizes task achievement. If α is large, the motor command magnitude is reduced at the expense of performance. The TOPS-α model is consistent with the current results in the sense that without the need for the greatest accuracy, subjects accept worse performance but with lower stiffness, resulting in reducing motor command magnitude. Slightly different movement duration and velocity profiles for different co-contraction levels may also suggest that desired trajectories were computed taking into account the magnitude of stiffness.

The results of our experiments suggest that the central nervous system somehow acquires the knowledge of the relationship between stiffness level and size of end-point deviation and error, allowing it to generate the stiffness necessary for difficult tasks. Furthermore, stiffness is reduced as long as the task demand is satisfied under skilled and natural movements. Optimal impedance control may be accomplished in order to generate the proper trajectory for the task requirements through a trade-off between the stiffness level and task achievement.

Generalization to multi-joint movements

The required movements were unnatural, and most subjects never rotated only the elbow without friction or gravity. There were three major reasons for this experimental setting. First, by minimizing the gravity and frictional forces during the movements, we could reliably estimate dynamic torques from surface EMG recordings. This was important for stiffness estimation via IMCJ. Second, by avoiding the shoulder freedom, we did not need to record from many shoulder muscles, thus shortening the experimental duration and simplifying the IMCJ computation. Finally, and most importantly, the hand path was forced to be identical between trials and subjects, and movement variability could result only from changes in velocity profiles. This is very important because we wanted to examine the effect of stiffness control on movement accuracy while minimizing changes in trajectory shapes. For multi-joint movements, it is known that the hand paths themselves fluctuate between trials and change systematically between subjects. Laursen et al. (1998) and Gribble et al. (2003) examined multi-joint movements and measured muscle activation by EMG activity for different accuracy requirements. Although, unlike us, they did not estimate joint stiffness and did not examine voluntary co-contraction, they found qualitatively similar results for the effects of accuracy requirements on co-contraction. Thus, we expect that at least a part of our results could be extended to more natural movements.

ACKNOWLEDGEMENTS

This study was supported by the Telecommunications Advancement Organization of

Japan and by grants to Mitsuo Kawato from the Human Frontier Science Program. We thank David Franklin for his valuable comments on the manuscript.

REFERENCES

Akazawa K. Modulation and adaptation of mechanical properties of mammalian skeletal muscle. In: *Clinical Biomechanics and Related Research,* edited by Hirasawa Y, Sledge CB, Woo SLY: Springer-Verlag, pp. 217-227, 1994.

Alexander RM. A minimum energy cost hypothesis for human arm trajectories, *Biol Cybern* 76: 97-105, 1997.

Bizzi E, Accornero N, Chapple W, and Hogan N. Posture control and trajectory formation during arm movement. *J Neurosci* 4: 2738-2744, 1984.

Burdet E, Osu R, Franklin D, Milner TE, and Kawato M. A method for measuring endpoint stiffness during multi-joint arm movements. *Journal of Biomechanics,* 33, 1705-1709, 2000.

Burdet E, Osu R, Franklin D, Milner T, and Kawato M. The central nervous system stabilizes unstable dynamics by learning optimal impedance. *Nature* 414: 446-449, 2001.

Clamman PH. Statistical analysis of motor unit firing pattern in human skeletal muscle. *Biophysics* J 9: 1233-1251, 1969.

Clancy EA and Hogan N. Probability density of the surface electromyogram and its relation to amplitude detectors. *IEEE Trans Biomed Eng* 46: 730-739, 1999.

Dul J, Johnson GE, Shiavi R, and Townsend MA. Muscular synergism—II. A minimum-fatigue criterion for load sharing between synergistic muscles. *J Biomch* 17: 675-684, 1984.

Darling WG and Cooke JD. Movement related EMGs become more variable during learning of fast accurate movements. *J Motor Behavior* 19: 311-331, 1987

Fitts PM. The information capacity of the human motor system in controlling the amplitude of movement. *J Exp Psychol* 47: 381-391, 1954.

Flash T and Hogan N. The coordination of arm movements: an experimentally confirmed mathematical model. *J Neurosci* 5: 1688-1703, 1985.

Franklin DW, Osu R, Burdet E, Kawato M, and Milner TE. Adaptation to stable and unstable environments achieved by combined impedance control and inverse dynamics model. *J Neurophysiol* 90: 3270-3282, 2003.

Gomi H and Kawato M. Equilibrium-point control hypothesis examined by measured arm-stiffness during multijoint movement. *Science* 272, 117-120, 1996.

Gomi H and Osu R. Task-dependent viscoelasticity of human multijoint arm and its spatial characteristics for interaction with environments. *J Neurosci*, 18: 8965-8978,

1998.

Gottlieb GL, Corcos DM, and Agarwall GC. Organizing principles for single-joint movements. I. A speed-insensitive strategy. *J Neuorphysiol*. 62: 342-357, 1989.

Gribble PL, Mullin LI, Cothros N, and Mattar A. Role of cocontraction in arm movement accuracy. *J Neurophysiol*. 89: 2396-405, 2003.

Hamilton A and Wolpert DM. Controlling the statistics of action: Obstacle avoidance. *J Neurophysiol* 87: 2434-2440, 2002.

Harris C and Wolpert DM. Signal-dependent noise determines motor planning. *Nature* 394: 780-784, 1998.

Hirayama M, Kawato M, and Jordan MI. The cascade neural network model and a speed-accuracy trade-off of arm movement. *J Motor Behav* 25: 162-174, 1993.

Hogan N. Adaptive control of mechanical impedance by coactivation of antagonist muscles. *IEEE Trans Auto Cont*. 29: 681-690, 1984.

Hogan N. The mechanics of multi-joint posture and movement control. *Biol Cybern* 52: 315-331, 1985.

Jones K, Hamilton A, and Wolpert DM. The sources of signal dependent noise during isometric force production. *J Neurophysiol* 88: 1533-1544, 2002.

Kawato M. Optimization and learning in neural networks for formation and control of coordinated movement. In: *Attention and Performance XIV*, edited by Meyer DE and Kornblum S: MIT Press, pp. 821-849, 1992.

Koike Y and Kawato M. Estimation of dynamic joint torques and trajectory formation from surface electromyography signals using a neural network model. *Biological Cybernetics* 73, 291-300, 1995.

Lacquaniti F, Carrozzo M, and Borghese NA. Time-varying mechanical behavior of multijointed arm in man. *J Neurophysiol* 69:1443-1464, 1993.

Laursen B, Jensen BR, and Sjogaard G. Effect of speed and precision demands on human shoulder muscle electromyography during a repetitive task. *Eur J Appl Physiol Occup Physiol* 78: 544-548, 1998.

Matthews PBC. Relationship of firing intervals of human motor unit to the trajectory of post-spike after-hyperpolarization and synaptic noise. *J Physiol* 492: 597-628, 1996.

McIntyre J, Mussa-Ivaldi FA, and Bizzi E. The control of stable postures in the multijoint arm. *Exp Brain Res* 110: 248-264, 1996.

Milner TE and Cloutier C. Compensation for mechanically unstable loading in

voluntary wrist movement. *Exp Brain Res* 94: 522-532, 1993.

Miyamoto H, Nakano E, Wolpert DM, and Kawato M. TOPS (Task Optimization in the Presence of Signal-dependent noise) model. *IEICE Trans Inf & Syst (Japanese Edition)* J85-DII: 940-949, 2002.

Miyamoto H, Wolpert DM, and Kawato M. Computation of optimal trajectory of arm movement with signal-dependent noise: the maximum task achievement model. In: *Biologically Inspired Robot Behavior Engineering*, edited by Dura RJ, Santos J, and Grana M: Physica-verlag, pp. 395-415, 2002.

Mussa-Ivaldi FA, Hogan N, and Bizzi E. Neural, mechanical, and geometric factors subserving arm posture in humans. *J Neurosci* 5:2732-2743, 1985.

Nagata Y, Miyamoto H, Nakano E, and Kawato M. Quantitative examinations of trajectory planning criteria in multijoint movement –TOPS model-. *Technical Report of the Institute of Electronics, Information and Communication Engineers*, NC2002-70, 25-35 (in Japanese) 2002.

Nakano E, Imamizu H, Osu R, Uno Y, Gomi H, Yoshioka T, and Kawato M. Quantitative examination of internal representations for arm trajectory planning: Minimum commanded torque change model. *J Neurophysiol* 81: 2140-2155, 1999.

Osu R, Burdet E, Franklin DW, Milner TE, and Kawato M. Different mechanisms involved in adaptation to stable and unstable dynamics. *J Neurophysiol* 90: 3255-3269, 2003.

Osu R, Franklin DW, Kato H, Gomi H, Domen K, Yoshioka T, and Kawato M. Short- and long-term changes in joint co-contraction associated with motor learning as revealed from surface EMG. *J Neurophysiol* 88: 991-1004, 2002.

Osu R and Gomi H. Multijoint muscle regulation mechanisms examined by measured human arm stiffness and EMG signals. *J Neurophysiol* 81: 1458-68, 1999.

Schmidt RA, Zelaznik H, Hawkins B, Frank JS, and Quinn, Jr. JT. Motor-output variability: A theory for the accuracy of rapid motor acts, *Psychol Rev* 86: 415-451, 1979.

Sherwood DE and Schmidt RA. The relationship between force and force variability in minimal and near-maximal static and dynamic contractions. *J Motor Behav* 12: 75-89, 1980.

Sherwood DE, Schmidt RA, and Walter CB. The force/force-variability relationship under controlled temporal conditions. *J Motor Behav* 20: 106-116, 1988.

St-Amant Y, Rancourt D, and Clancy EA. Influence of smoothing window length on

electromyogram amplitude estimates. *IEEE Trans Biomed Eng* 45: 795-799, 1998.

Todorov E and Jordan M. Optimal feedback control as a theory of motor coordination. *Nature Neuroscience* 5: 1226-1235, 2002.

Tsuji T, Morasso PG, Goto K, and Ito K. Human hand impedance characteristics during maintained posture, *Biol Cybern* 72: 475-485, 1995.

Uno Y, Kawato M, and Suzuki R. Formation and control of optimal trajectory in human multijoint arm movement: Minimum torque-change model. *Biol Cybern* 61: 89-101, 1989.

Wada Y, Kaneko Y, Nakano E, Osu R, and Kawato M. Quantitative examinations for multi joint arm trajectory planning -- using a robust calculation algorithm of the minimum commanded torque change trajectory --. *Neural Networks* 14: 381-393, 2001.

Figure Legends

Fig. 1 (A) Experimental setup and CRT display patterns for changed target-size experiment (B) and voluntary co-contraction control experiment (C). The two arm positions shown in (A) indicate either the start or end position depending on extension or flexion movements. The CRT display patterns of (B) and (C) show extension movement. In the EMG level display of (C), the two extensor-muscle activities are shown on the right and the two flexor-muscle activities are shown on the left by the x marks.

Fig. 2 EMG deviation at each time point plotted against EMG magnitude at that time point for a typical subject during voluntary co-contraction experiment. Green, red, and blue dots denote high, medium, and low co-contraction conditions, respectively. Upper four panels are plots for extension movements and lower four are those for flexion movements. Middle four panels (cyan background) are plots when muscles are working as agonists. The other four panels (magenta background) are plots when muscles are working as antagonists.

Fig. 3 Histograms of the slopes between EMG magnitude and EMG deviation estimated for each muscle of each subject. Upper two panels are histograms of target-size experiments and lower two are those of co-contraction experiments. Vertical lines denote slopes of uniform, Gaussian, and Laplace distributions.

Fig. 4 Results of a typical subject for the target-size experiment for extension movements. The results for large, medium and small target sizes are shown in the left, middle, and right columns, respectively. (A) shows the hand paths and end-point distributions. (B), (C) and (E) show velocity profiles, torque profiles, and stiffness profiles, respectively, as a function of time for 40 trials shown by thin gray curves. Ensemble-averaged time courses are indicated by solid colored curves. (D) shows the average EMG time courses of the four muscles. Ensemble averaging equations for C to E are given in Materials and Methods.

Fig. 5 Ensemble-averaged time courses across all subjects and all trials classified by

target size shown by three colors: blue for large, red for medium, and green for small target size. (A), (B), (C), and (D) show the summed EMG activity over the four muscles, stiffness, torque, and velocity. (E), (F), and (G) show the ensemble-averaged deviations across all subjects for the summed EMG activity, torque, and position, respectively. (H) shows a magnification of (G) around the end of movement. The data from extension (upper panel) and flexion (lower panel) are shown separately.

Fig. 6 RMS EMG of each muscle for each subject and movement direction against target size. Large, Medium, and Small indicate large, medium and small target sizes, respectively. The open circles indicate flexion movements, and the crosses extension movements. The p-values in each panel denote results of repeated measures ANOVA among target sizes ($F(2,16) = 6.98$ for elbow flexor, $F(2,16) = 10.04$ for biarticular flexor, $F(2,16) = 12.52$ for elbow extensor, $F(2,16) = 6.74$ for biarticular extensor). The horizontal bars denote significant comparison in post-hoc test (Tukey's HSD test; $P < 0.05$).

Fig. 7 Means and standard deviations (vertical bars) of six indices across all subjects for each target size. Large, Medium, and Small indicate large, medium and small target sizes, respectively. The gray lines denote extension data, and the black lines denote flexion data. The horizontal lines indicate significant comparisons. An interaction between target size and movement direction was significant for all indices except end-point deviation ($P < 0.01$). A and B show the means and standard deviations across subjects for the summed EMG activity and stiffness, respectively, which were time-averaged over the entire movement duration. C, D, and E show the means and standard deviations of the deviations that were time-averaged over the entire movement duration for EMG activity, torque, and position, respectively. F shows the mean and standard deviation of the end-point deviation. See Materials and Methods for the equations used to calculate the time-averaged deviations in C to E.

Fig. 8 Results of the same subject shown in Fig. 4 for the voluntary co-contraction control experiment for extension movements. The results for the normal, medium and high levels of co-contraction are shown in the left, middle, and right columns, respectively. The format is similar to Fig. 4. (A) shows the hand paths and end-point distributions.

(B), (C), and (E) show velocity profiles, torque profiles, and stiffness profiles, respectively, as a function of time for 40 trials, and ensemble-averaged time courses are indicated by solid colored curves. (D) shows the average EMG time courses of the four muscles.

Fig. 9 Ensemble-averaged time courses across all subjects and all trials classified by co-contraction levels shown by three colors: blue for normal, red for medium, and green for high in a similar format to Fig. 5. (A), (B), (C), and (D) show the summed EMG activity over the four muscles, stiffness, torque, and velocity. (E), (F), and (G) show the ensemble-averaged deviations across all subjects for the summed EMG activity, torque, and position, respectively. (H) shows a magnification of (G) around the end of movement. The data from extension (upper panel) and flexion (lower panel) are shown separately.

Fig. 10 Means and standard deviations (vertical bars) of six indices across all subjects for each co-contraction level in a similar format to Fig. 7. Norm, Med and High indicate normal, medium and high co-contraction levels, respectively. The gray lines denote extension, and the black lines denote flexion data. The horizontal lines indicate significant comparisons. An interaction between co-contraction level and movement direction was significant for summed EMG, EMG, torque and position deviation ($P < 0.01$). A and B show the summed EMG activity and stiffness, respectively, which were time-averaged over the entire movement duration. C, D, and E show means and standard deviations of the deviations that were time averaged over the entire movement duration for EMG activity, torque, and position, respectively. F shows the mean and standard deviation of the end-point deviation. G shows the mean and standard deviation of the end-point error.

Fig. 11 Plots of correlation coefficients between the stiffness and variabilities of five quantities for all subjects. A is for the voluntary co-contraction control experiment and B is for the target-size experiment. The circles show extension coefficients and the squares show flexion coefficients. Coefficients from the same subject are connected by a thin line. The bold line with asterisks shows the correlation coefficients that were calculated from all trials of all subjects for both flexion and

extension data. The EMG deviation (leftmost) shows the correlation coefficients between EMG activity and EMG variability. The torque deviation (second from left) shows the correlation coefficients between stiffness and torque variability. The position deviation (middle) shows the correlation coefficients between stiffness and position variability. The end-point deviation (second from right) shows the correlation coefficients between stiffness and end-point deviation. The end-point error (rightmost) shows the correlation coefficients between stiffness and end-point error. The dark shaded regions show the range of statistical insignificance, outside of which the correlation coefficients computed from all trials of all subjects are statistically significantly different from zero. The light shaded region is the insignificance range for an individual subject.

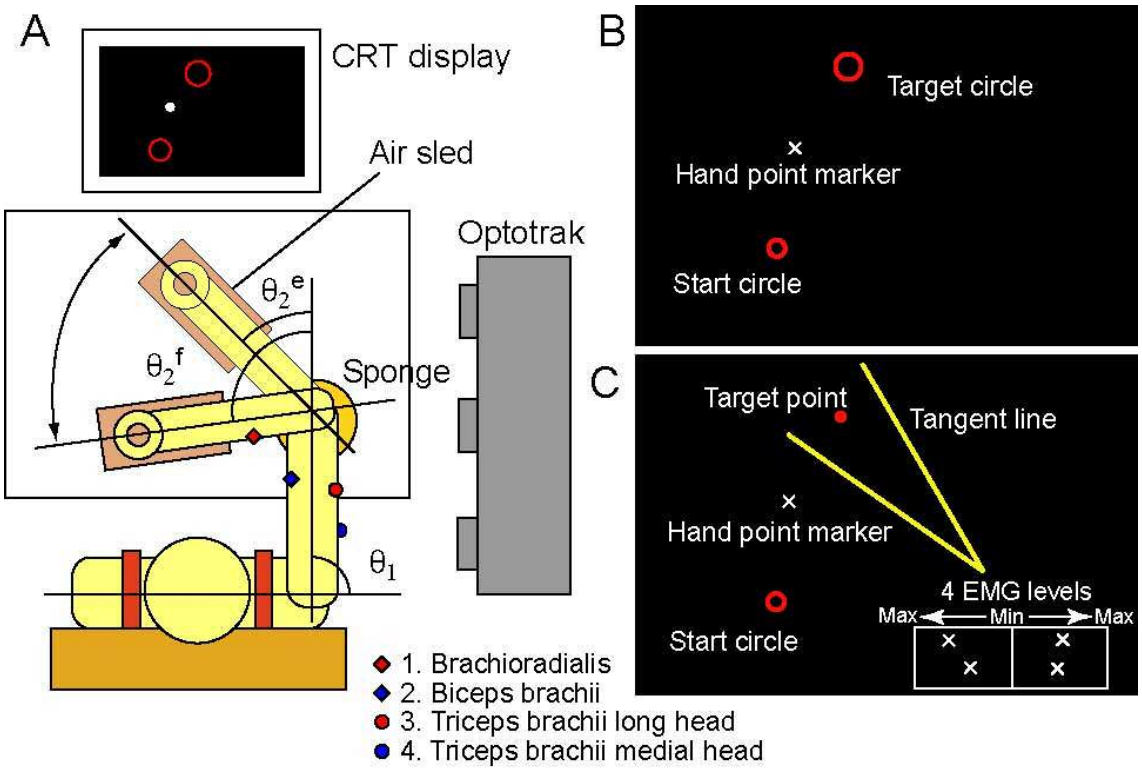
A
CRT display
Air sled
Optotrak
θ_2^e
θ_2^f
Sponge
θ_1
B
Target circle
Hand point marker
Start circle
C
Target point
Tangent line
Hand point marker
4 EMG levels
Max
Min
Max
Start circle
1. Brachioradialis
2. Biceps brachii
3. Triceps brachii long head
4. Triceps brachii medial head

Figure 1

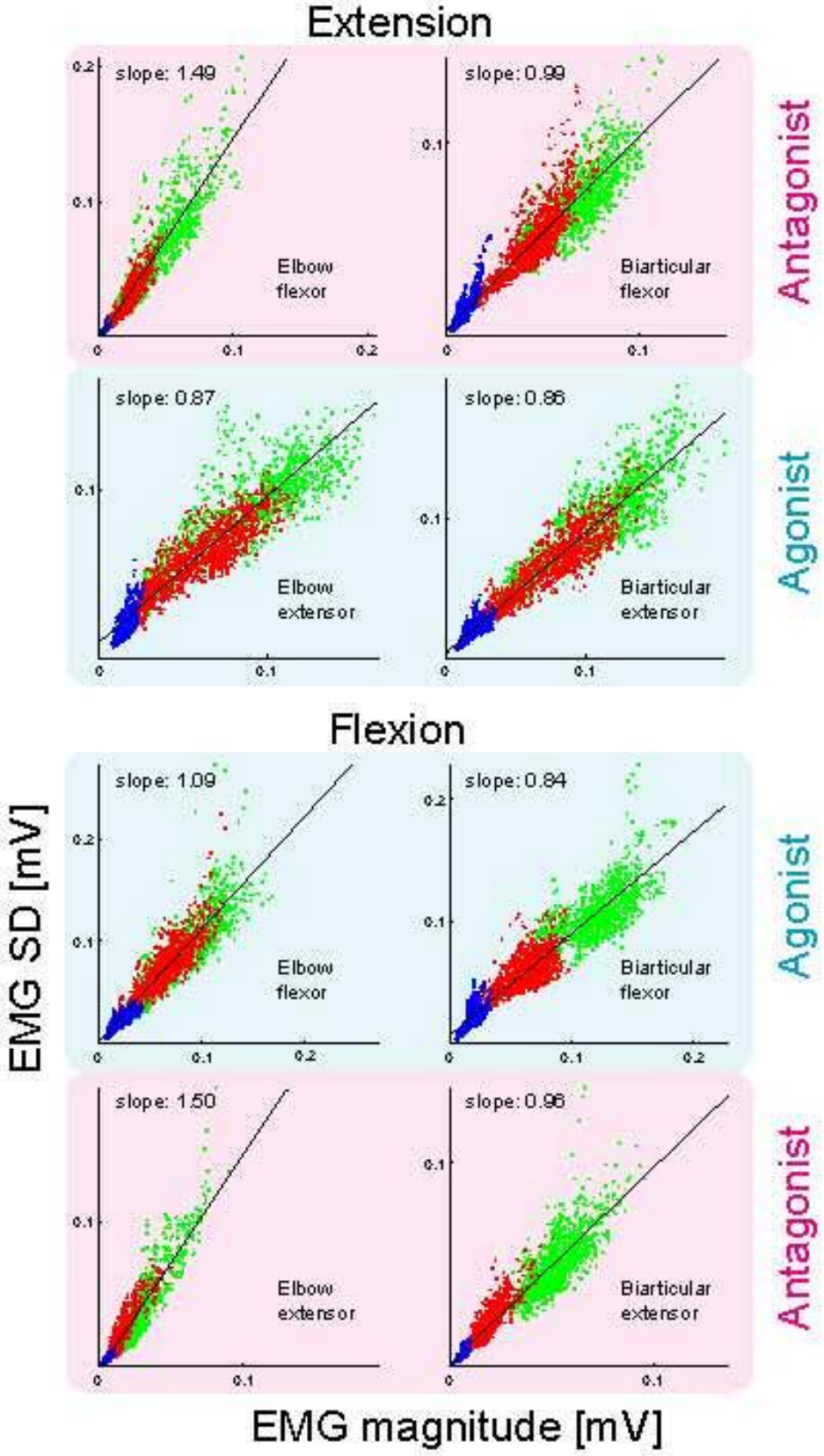
Extension
slope: 1.49
Elbow flexor
slope: 0.99
Biarticular flexor
Antagonist
slope: 0.87
Elbow extensor
slope: 0.86
Biarticular extensor
Agonist
Flexion
slope: 1.09
Elbow flexor
slope: 0.84
Biarticular flexor
Agonist
slope: 1.50
Elbow extensor
slope: 0.96
Biarticular extensor
Antagonist
EMG SD [mV]
EMG magnitude [mV]

Figure 2

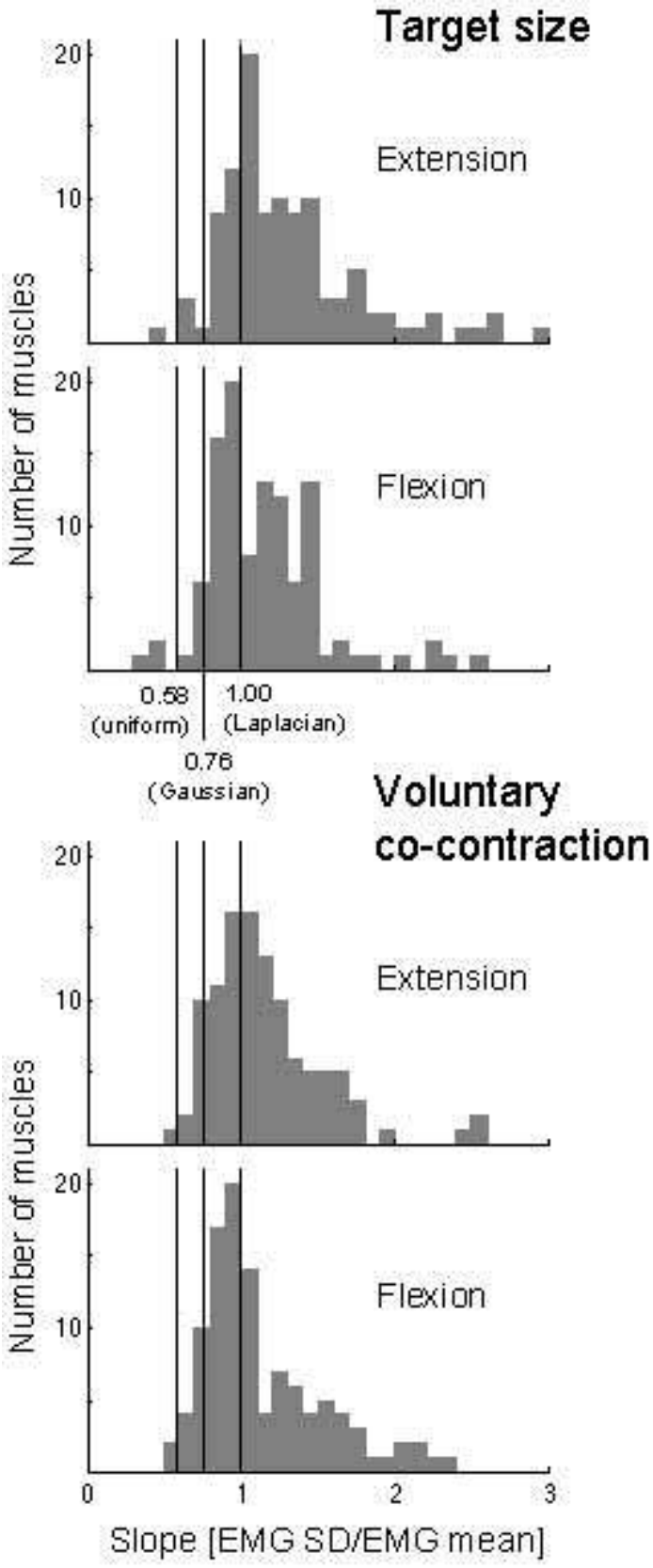
Target size
Extension
Flexion
Number of muscles
20
10
0.58
(uniform)
1.00
(Laplacian)
0.76
(Gaussian)
Voluntary
co-contraction
Extension
Flexion
Number of muscles
0
1
2
3
Slope [EMG SD/EMG mean]

Figure 3

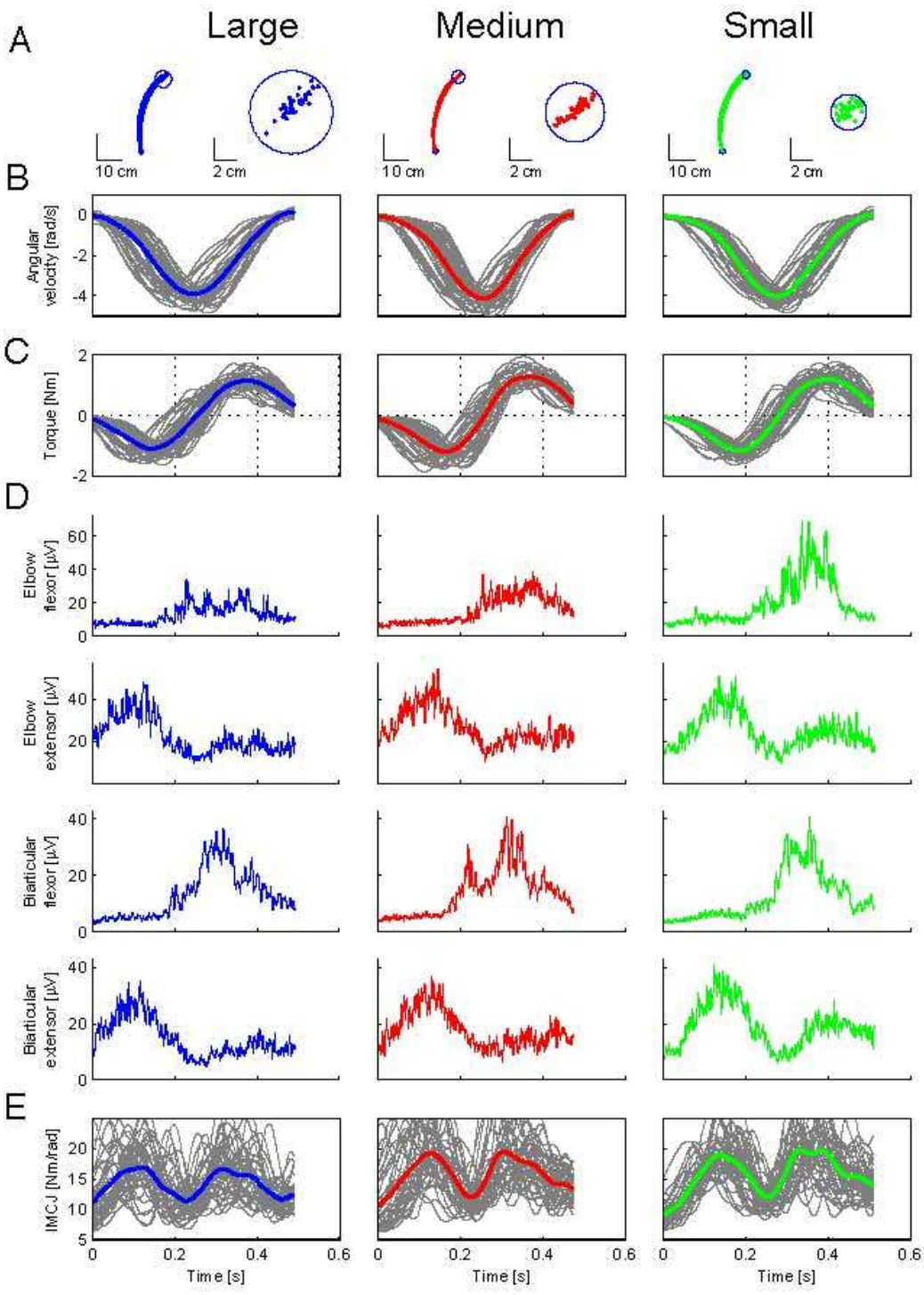
A
Large
Medium
Small
10 cm
2 cm
B
Angular velocity [rad/s]
C
Torque [Nm]
D
Elbow flexor [μV]
Elbow extensor [μV]
Biarticular flexor [μV]
Biarticular extensor [μV]
E
IMCJ [Nm/rad]
Time [s]

Figure 4

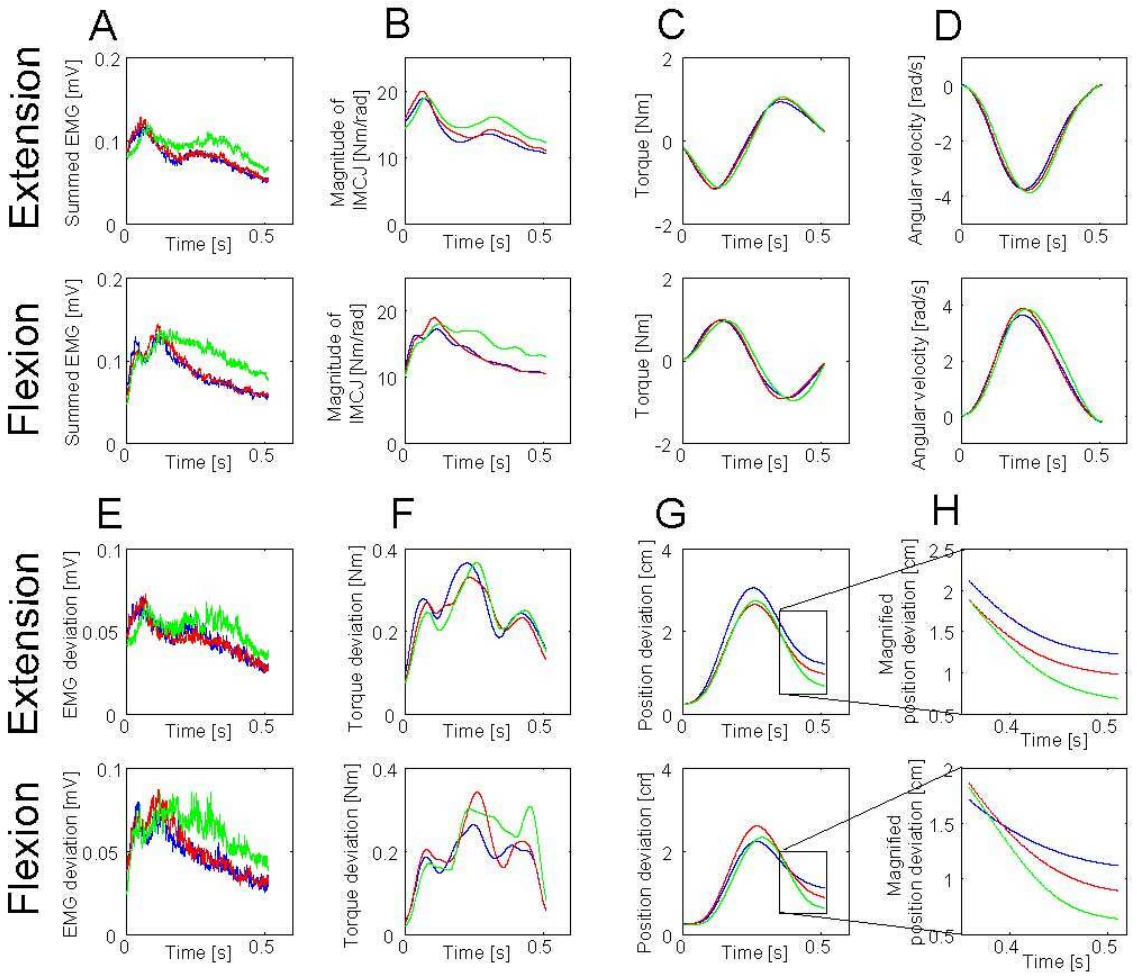
A
B
C
D
Extension
Flexion
Summed EMG [mV]
Magnitude of IMCJ [Nm/rad]
Torque [Nm]
Angular velocity [rad/s]
Time [s]
E
F
G
H
EMG deviation [mV]
Torque deviation [Nm]
Position deviation [cm]
Magnified position deviation [cm]

Figure 5

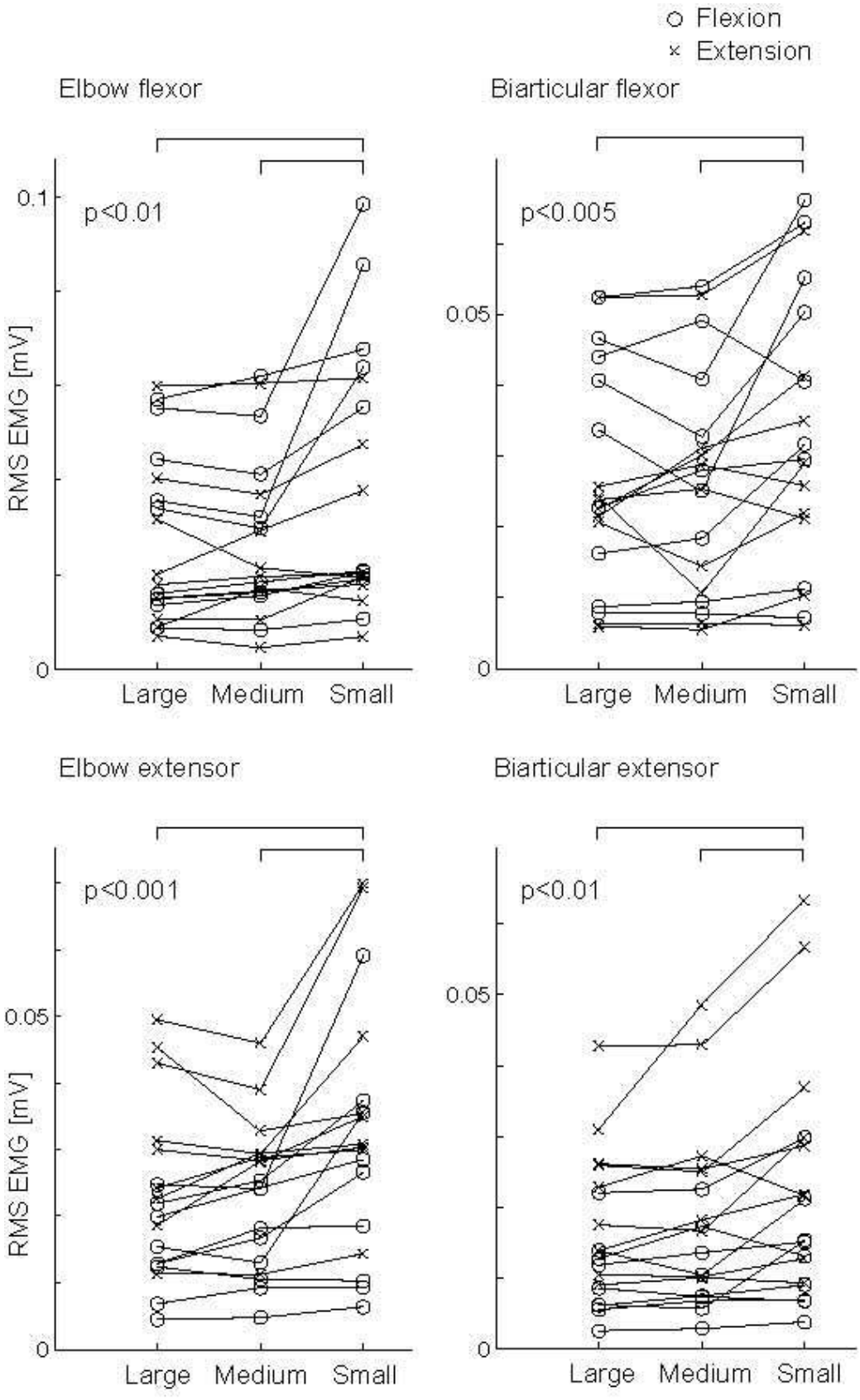
Flexion
Extension
Elbow flexor
Biarticular flexor
Elbow extensor
Biarticular extensor
RMS EMG [mV]
p<0.01
p<0.005
p<0.001
p<0.01
0.1
0.05
0
Large
Medium
Small

Figure 6

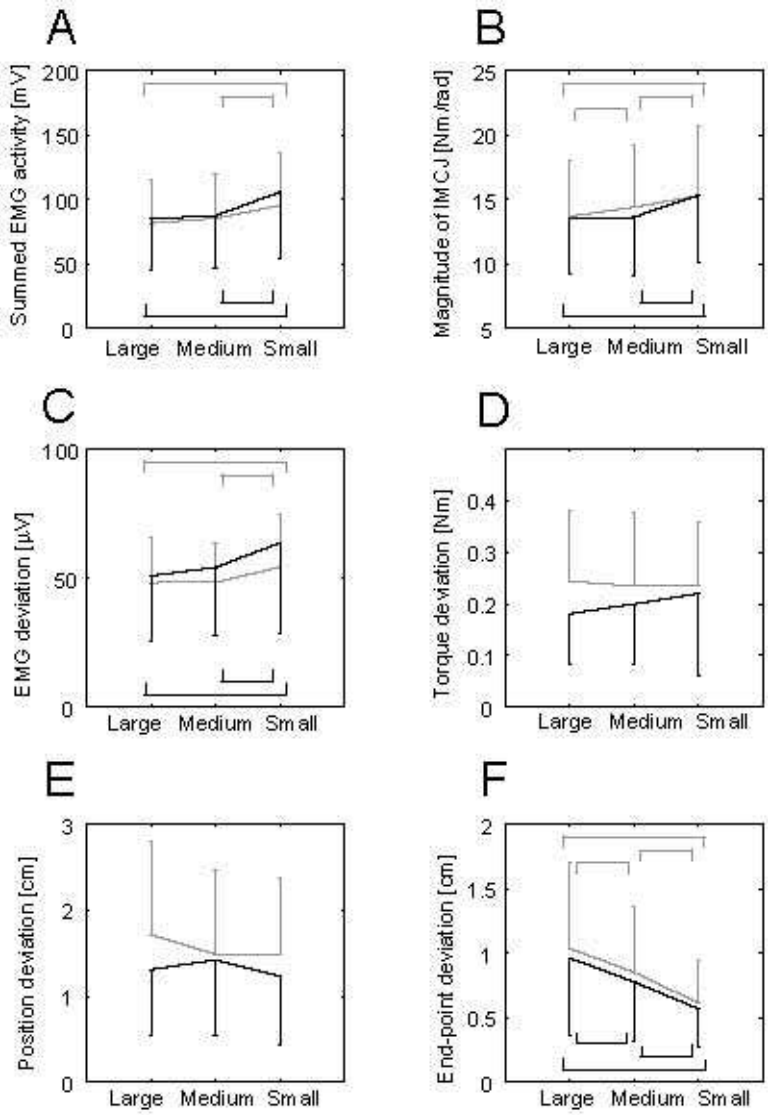
A
Summed EMG activity [mV]
200
150
100
50
0
Large Medium Small
B
Magnitude of IMCJ [Nm/rad]
25
20
15
10
5
Large Medium Small
C
EMG deviation [µV]
100
50
0
Large Medium Small
D
Torque deviation [Nm]
0.4
0.3
0.2
0.1
0
Large Medium Small
E
Position deviation [cm]
3
2
1
0
Large Medium Small
F
End-point deviation [cm]
2
1.5
1
0.5
0
Large Medium Small

Figure 7

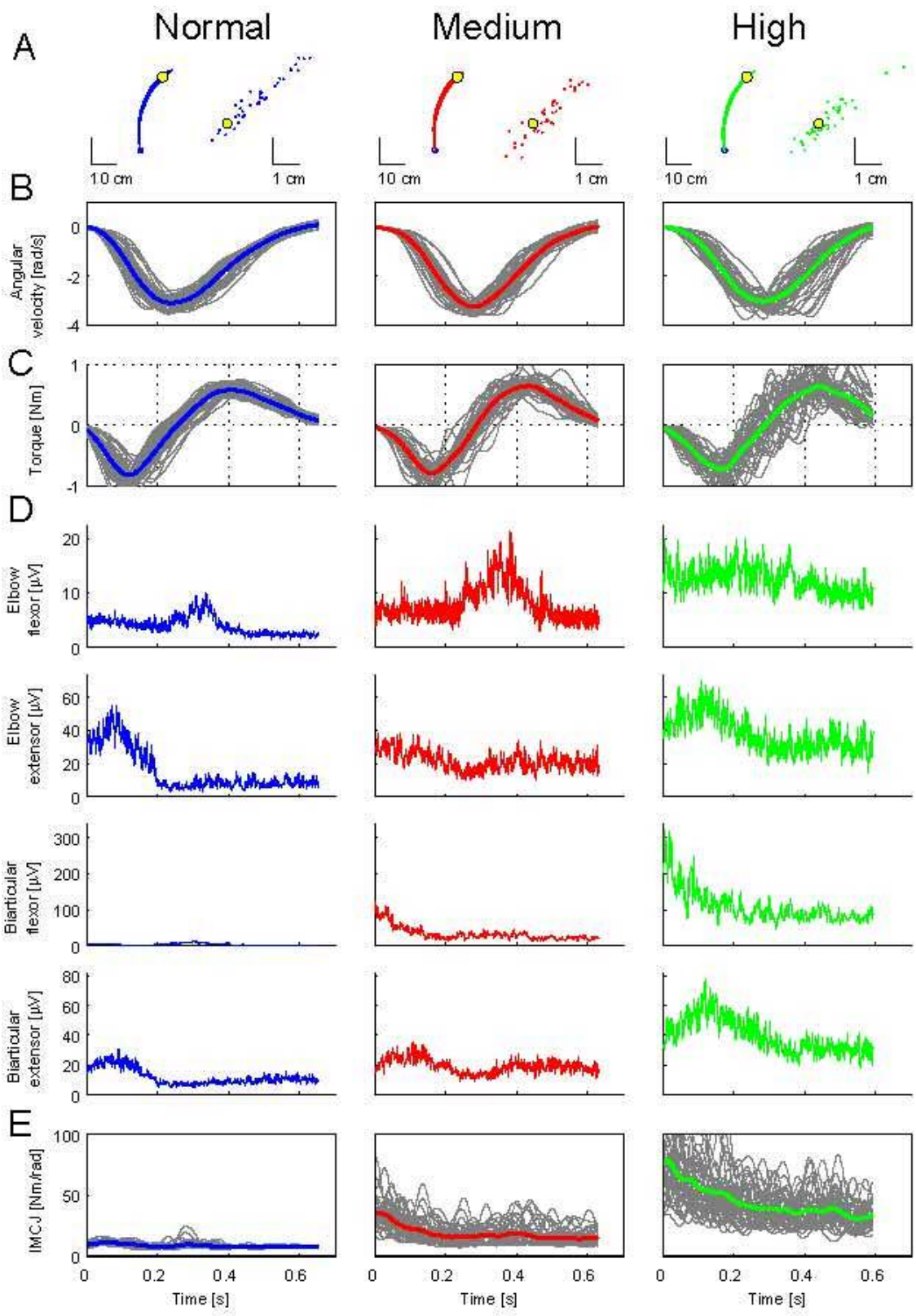
Normal
Medium
High
A
10 cm
1 cm
B
Angular velocity [rad/s]
C
Torque [Nm]
D
Elbow flexor [μV]
Elbow extensor [μV]
Biarticular flexor [μV]
Biarticular extensor [μV]
E
IMCJ [Nm/rad]
Time [s]

Figure 8

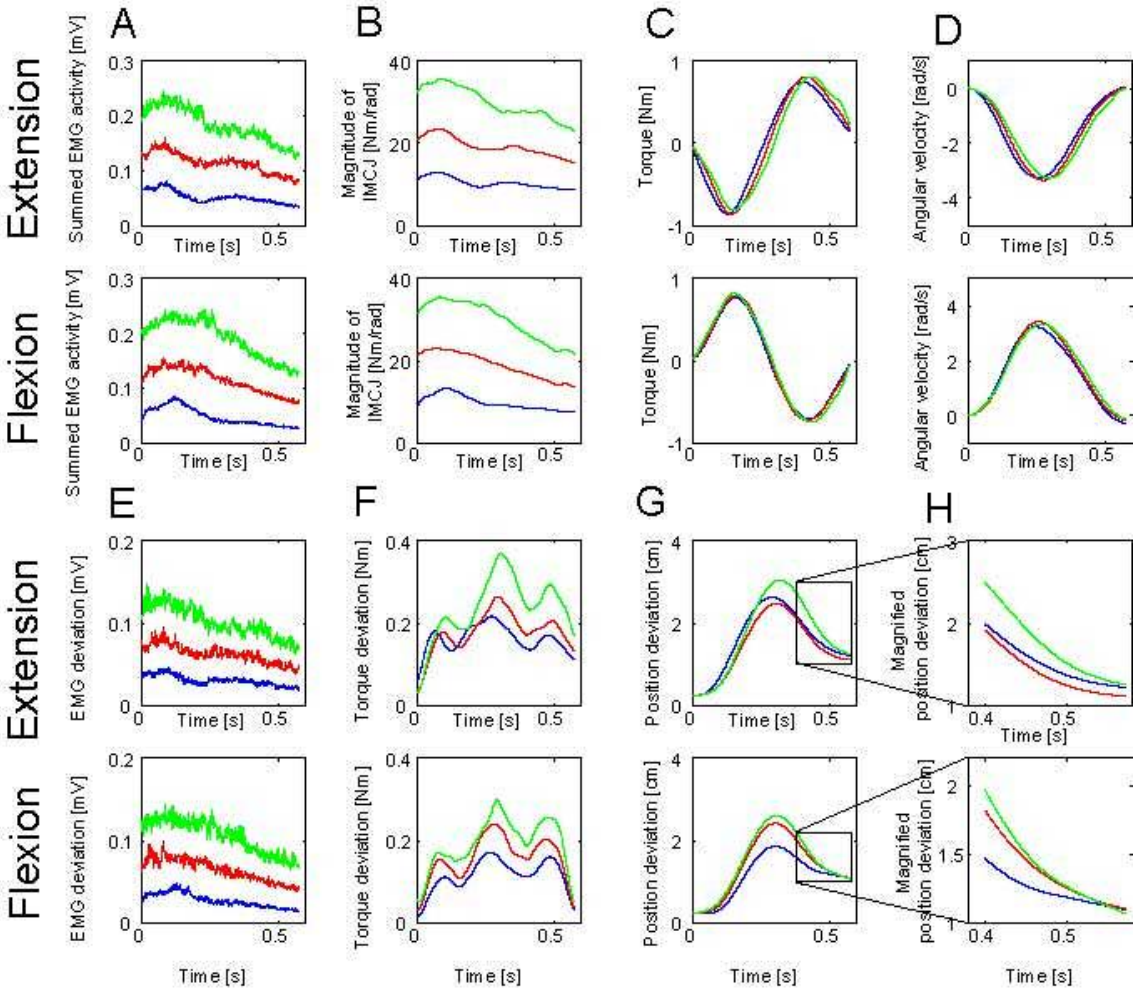
Extension
Flexion
Extension
Flexion
A
B
C
D
E
F
G
H
Summed EMG activity [mV]
Magnitude of IMCJ [Nm/rad]
Torque [Nm]
Angular velocity [rad/s]
EMG deviation [mV]
Torque deviation [Nm]
Position deviation [cm]
Magnified position deviation [cm]
Time [s]

Figure 9

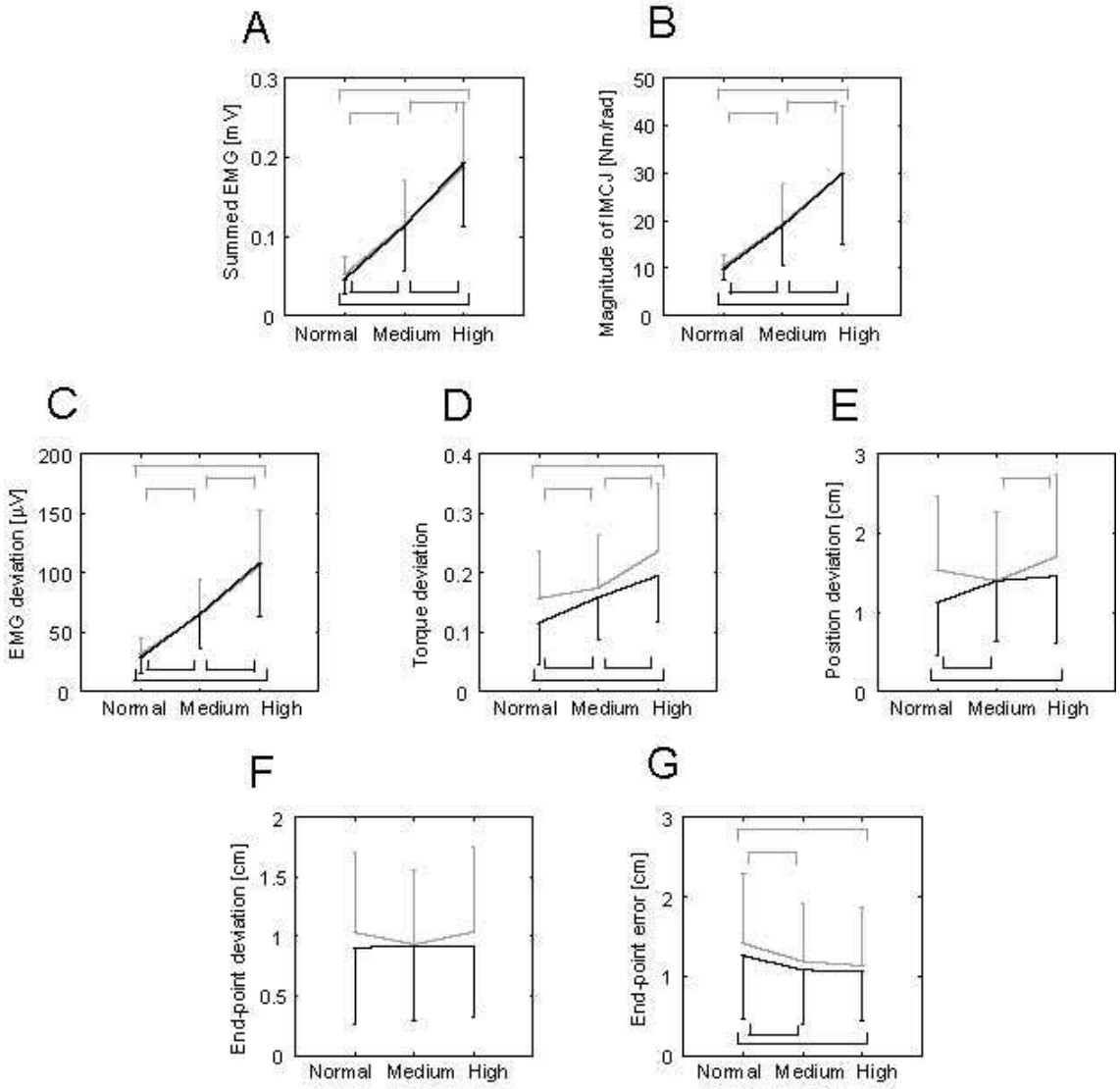
A
Summed EMG [mV]
0.3
0.2
0.1
0
Normal Medium High
B
Magnitude of IMCJ [Nm/rad]
50
40
30
20
10
0
Normal Medium High
C
EMG deviation [µV]
200
150
100
50
0
Normal Medium High
D
Torque deviation
0.4
0.3
0.2
0.1
0
Normal Medium High
E
Position deviation [cm]
3
2
1
0
Normal Medium High
F
End-point deviation [cm]
2
1.5
1
0.5
0
Normal Medium High
G
End-point error [cm]
3
2
1
0
Normal Medium High

Figure 10

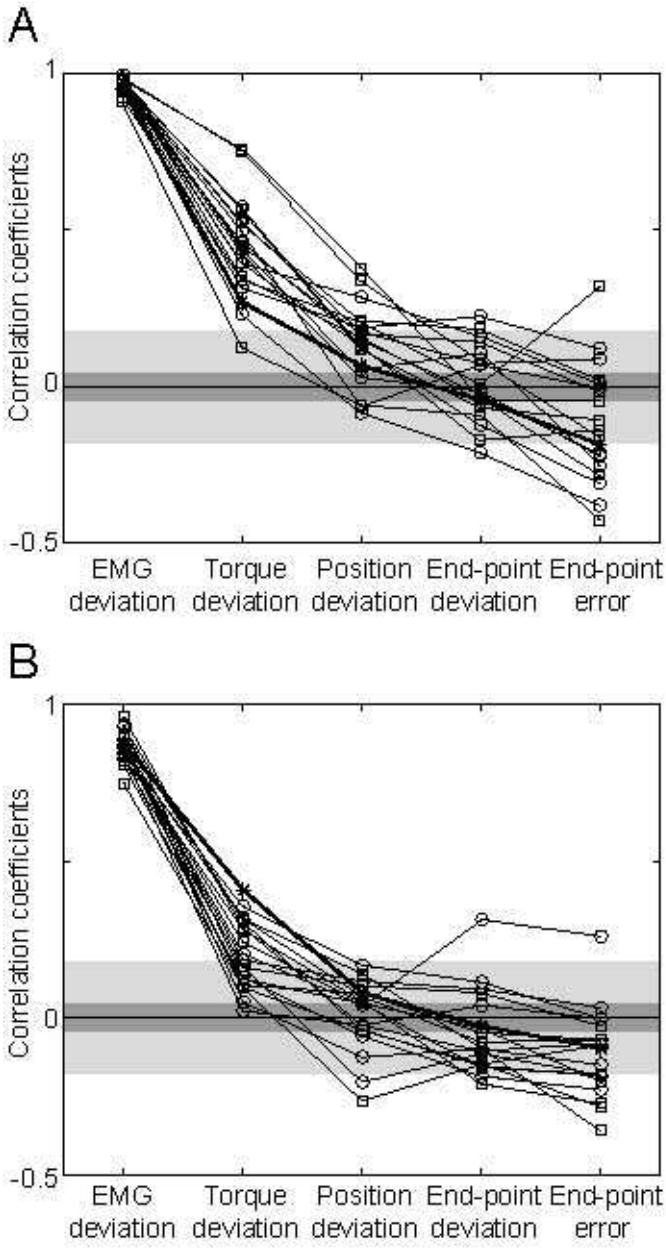
A
1
0
-0.5
Correlation coefficients
EMG deviation
Torque deviation
Position deviation
End-point deviation
End-point error
B
1
0
-0.5
Correlation coefficients
EMG deviation
Torque deviation
Position deviation
End-point deviation
End-point error

Figure 11